LBL-17149
c.2

Lawrence Berkeley Laboratory
UNIVERSITY OF CALIFORNIA

RECEIVED
LAWRENCE
BERKELEY LABORATORY

JUL 6 1984

LIBRARY AND
DOCUMENTS SECTION

CELL PROLIFERATION KINETICS AND RADIATION RESPONSE
IN 9L TUMOR SPHEROIDS

S.E. Sweigert
(Ph.D. Thesis)

May 1984

TWO-WEEK LOAN COPY

This is a Library Circulating Copy
which may be borrowed for two weeks.
~~For a personal retention copy, call~~
~~Tech. Info. Division, Ext. 6782~~.

Donner Laboratory
Biology & Medicine Division

LBL-17149
c.2

Prepared for the U.S. Department of Energy under Contract DE-AC03-76SF00098

DISCLAIMER

This document was prepared as an account of work sponsored by the United States Government. While this document is believed to contain correct information, neither the United States Government nor any agency thereof, nor the Regents of the University of California, nor any of their employees, makes any warranty, express or implied, or assumes any legal responsibility for the accuracy, completeness, or usefulness of any information, apparatus, product, or process disclosed, or represents that its use would not infringe privately owned rights. Reference herein to any specific commercial product, process, or service by its trade name, trademark, manufacturer, or otherwise, does not necessarily constitute or imply its endorsement, recommendation, or favoring by the United States Government or any agency thereof, or the Regents of the University of California. The views and opinions of authors expressed herein do not necessarily state or reflect those of the United States Government or any agency thereof or the Regents of the University of California.

LBL-17149

CELL PROLIFERATION KINETICS AND RADIATION RESPONSE IN 9L TUMOR SPHEROIDS

Susan Elaine Sweigert
Ph.D. Thesis

Biology and Medicine Division
Lawrence Berkeley Laboratory
University of California
Berkeley, California 94720

May 1984

This work was supported by the U.S. Department of Energy under Contract Number DE-AC03-76SF00098.

ABSTRACT

Cell kinetic parameters, including population doubling-time, cell cycle time, and growth fraction, were measured in 9L gliosarcoma spheroids (an *in vitro* tumor model). These parameters were studied as the spheroids grew from 50 μm to over 900 μm in diameter. Experiments relating the cell kinetic parameters to the radiation response of 9L spheroids were also carried out. The major findings were these: 1) The average cell cycle time (T_c), is considerably longer in large spheroids than in exponentially-growing monolayers. 2) The radiosensitivity of noncycling (but still viable) cells in spheroids is not significantly different from that of cycling spheroid cells; the presence of a noncycling subpopulation cannot account for the radioresistance of cells grown as spheroids compared to monolayer cells. 3) Radiation-induced division delay (RIDD) is approximately twice as long in spheroid cells as in monolayer cells given equal radiation doses. Finally, the cell loss factor for spheroids of various sizes was calculated, by using the measured kinetic parameters in the basic equations for growth of a cell population.

The technique of pulse-labelled mitoses (PLM) was used to estimate T_c in exponential monolayers, 400 μm and 800 μm diameter spheroids. Values obtained were, respectively, 16.6 hours, 24 hours and 28 hours. Growth fractions (GFs) were determined by two independent techniques, both involving ^{3}H-thymidine labelling and autoradiography. First, as the labelling-index of spheroids labelled continuously over an interval equal to the duration of $G_2 + M + G + 2$ hr. Second, by

using the values of T_s, T_c, and the pulse-labelling-index from the PLM data. The GF declined from 0.86 in spheroids <150 μm to 0.5 in 500 μm spheroids; GF remained approximately 0.5 in spheroids up to 850 μm in diameter.

T_D's (spheroid doubling-times) were determined from a curve of number of cells per spheroid vs. days in culture, by estimating tangents to the curve at points corresponding to various spheroid sizes. Overall, the growth curve could be divided into three regions. Below 200 μm, growth was exponential with T_D = 19 hours. A sharp increase in T_D to 28 hrs at 225-250 μm marked the beginning of the 'middle' region of growth, where T_D increased more gradually to 54 hours in 500-600 μm spheroids. The 'late' region was marked by another relatively sharp increase in T_D, to 91 hours in 700 μm spheroids. Beyond this T_D continued to increase, reaching 139 hours at 900 μm. Growth rate patterns in the three regions could be correlated with the kinetic parameters. In the early region, GF was high, and growth was exponential, similar to exponential growth in monolayers. In the middle region (200-600 μm) the progressive increase in T_D is ascribed to a decreasing GF and lengthening of T_c (cell cycle time), with relatively little cell loss. The late region (beyond 600 μm diameter) is marked by a sharp increase in cell loss due to cell death (see below) and a further lengthening of T_c, with little change in GF between 500 μm and 800 μm.

Cell loss factor ϕ was calculated from the relation $\phi = K_L/K_p$, where K_L = rate constant for cell loss and K_p = rate constant for cell production. The rate of cell shedding was measured and compared to the K_L calculated from the other kinetic parameters. ϕ was <0.15 for spheroids of diameter $\leq$500 μm; in this range cell loss was largely accounted for by cell shedding. For 800 μm spheroids, ϕ was 0.5 and only 1/3 or less of the total cell loss could be accounted for by cell shedding; the remainder was presumably due to cell death within the spheroid.

All of the results described above were obtained in cultures in which the cell density (in terms of number cells/ml medium) was kept at 1.5×10^5 cells/ml in order to avoid changes in the overall amount of nutrients available per cell. In a comparative study of T_D in cultures where cell density increased with spheroid growth and exceeded 10^5 cells/ml by size 450 μm, the onset of the 'late' region occurred earlier, at a diameter of 400-450 μm. Growth in the early and middle regions was indistinguishable from that of the density-controlled cultures. No kinetic parameters other than T_D were studied for the 'high-density' cultures.

Radiosensitivity of noncycling cells was studied in 800 μm spheroids using a "suicide" technique, whereby cycling cells were killed by 16-20 hours exposure to high-specific activity ^{3}H-thymidine. Following suicide treatment, spheroids were irradiated, dissociated and plated for the colony-formation assay of clonogenic survival.

Radiation survival of suicide-treated spheroids was compared to that of untreated spheroids; no significant difference was found.

The final studies compared radiation-induced division delay (RIDD) in 9L spheroids (800 μm) and monolayers, using the technique of pulse-labelled mitoses. Two doses were used, 500 rad and 800 rad. The RIDD was approximately twice as long in spheroid cells as in monolayers for equal doses: 4.3 hours vs. 2 hr. for 500 rad, 5.2 hr vs. 2.9 hr. for 800 rad doses. This increased RIDD for spheroids is not related to increased cell killing, since spheroid cell survival was greater than that for monolayer cells at each dose. In light of the current notion that RIDD represents a period of cell recovery, it is suggested that the longer RIDD in spheroids may be a factor in the enhanced radiation survival of 9L spheroid cells as compared to monolayers.

ACKNOWLEDGEMENTS

I want to express my special gratitude to two persons who aided me during my career as a graduate student in ways I can never properly repay. They are Dr. Edward Alpen, my research advisor, and Dr. Cornelius Tobias. Their confidence in me during some difficult times helped me to find the spirit to keep on going. My thanks also to my colleague Lynn Hlatky, for her very helpful discussions during the preparation of this dissertation. Finally, I am grateful to the UC Karate Club and its members who have been, outside of my work, the most constant and sustaining presence in my life during the three years in which this work was done.

This manuscript is dedicated to my family, especially my parents and my sister, without whose loyalty and support (moral and sometimes financial) I might not have gotten this far. In particular, to my mother, who gave me, through some combination of inheritance and early training, the qualities of independence, endurance and diligence without which I could not have achieved success.

TABLE OF CONTENTS

ABSTRACT iii

ACKNOWLEDGEMENTS vii

INTRODUCTION 1

I. Spheroids as a Tumor Model 1

II. Cell Proliferation in Mammalian Cell Systems 4

A. The Cell Cycle 4

B. Quiescent Cells 6

C. Kinetic Parameters of Cell Populations 13

D. Cell Proliferation in Spheroids 17

III. Radiobiology of Mammalian Cells 21

A. Radiation Cell Killing 21

B. Radiation-Induced Division Delay 27

C. Radiation Responses of Spheroids 28

IV. Rationale 33

MATERIALS AND METHODS 36

A. 9L Cells and Stock Cultures 36

B. Spheroid Culture and Manipulations 37

C. Tritium Labelling Experiments 40

D. Colony Formation Assay 44

E. Irradiations 45

RESULTS 46

I. Spheroid Growth Kinetics 46

A. Spheroid Growth Rates 46

B. Cell Cycle Parameters 48

C. Growth Fraction 49

D. Cell Shedding 50

II. Spheroid Radiation Response 50

A. Suicide Experiments 50

B. Post-Irradiation Cell Cycle Progression 51

DISCUSSION. 53

I. Spheroid Cell Population Kinetics 53

A. Measured Kinetic Parameters 53

B. Estimation of Cell Loss Factor. . . . . .

C. Summary: Dynamics of Spheroid Growth. 68

II. Spheroid Radiation Studies. 71

A. Radiosensitivity of Quiescent Cells 71

B. Radiation-Induced Division Delay. 73

C. G_2-Delay and Cell Survival. 77

APPENDIX. 80

BIBLIOGRAPHY. 81

FIGURES LEGENDS 100

TABLE LEGENDS 103

FIGURES 104

TABLES. 110

INTRODUCTION

I. SPHEROIDS AS A TUMOR MODEL

Spheroids were developed as a tumor model by Sutherland, McCredie and Inch (1). They are nonclonal aggregates of tumor cells up to 2-3 mm in diameter, which resemble regions found in nodular carcinomas *in vivo* (1). Such solid tumors contain nodules which are well-vascularized in peripheral regions, but have central necrotic zones at distances greater than 150 μm from blood vessels (2,3). Intermediate between the necrotic zone and the periphery of actively cycling cells is a region of slowly proliferating or nonproliferating cells. Histologically, mature spheroids (diameter of >400 μm) resemble these tumor nodules, having the three types of regions described above (1). In both spheroids and nodular carcinomas, the depth of viable cells corresponds roughly to the diffusion distance of oxygen in tissue (3,52). (Oxygen diffusion distance in tissues is limited by the O_2 consumption of cells closest to the supply.)

Spheroids originate as aggregates of 5-10 cells, which then grow by proliferation, possibly accompanied by continuing aggregation of cells on the surface. As they increase in diameter beyond 150-250 μm, they develop a central region of slowly proliferating or non-proliferating cells and eventually (300-400 μm diameter), a necrotic core (1,4). Overall there is a shift of cells into G_1 or a G_1-like quiescent state; this redistribution can affect both the radiation response and growth rates (4). The cell population doubling time,

T_D (as distinguished from the cell cycle time for individual cells, abbrev. T_c), increases to as much as 5-45 times the T_D of an exponentially growing monolayer. Tumors in vivo have a similar progressive slowing of the growth rate (5). This retardation of growth rates is due to the reduced fraction of proliferating cells and to cell loss. Cell loss includes both cell death in hypoxic and/or starved regions and migration of cells out of the system. Spheroids shed cells into the medium (73); this may be analogous to the shedding of cells into the blood or lymphatic system by tumors, which is the first step of metastasis.

Spheroids also resemble tumors in their radiation response. Cells are more resistant if irradiated as intact spheroids instead of as exponential cultures (4). Tumor cells are also more resistant if irradiated in vivo than if irradiated as single cells in vitro (6,7). Spheroids, like tumors, may contain a subpopulation of hypoxic cells, which are quite radioresistant compared to oxic cells. In addition, many assays which are used to study tumor radioresponse in vivo such as volume regression, regrowth, and tumor-cure dose, can be adapted for spheroids (8,9).

Most in vitro studies of radiobiology and toxicology have been done using either monolayer or single-cell suspension cultures. Spheroid cell populations differ in many respects from monolayer populations. A spheroid contains an oxygen gradient, nutrient gradients and probably a pH gradient. Accumulation of toxic metabolites may affect cells in inner regions. Monolayer cultures, on the other hand, are homogeneous

with respect to these factors. Some of these factors, especially hypoxia and lowered pH, are known to be important in the radiation response of tumors (10-12). Like tumors, spheroids contain a portion of noncycling but viable cells, which under the right conditions can be recruited back into the proliferating state. Exponentially-growing monolayers do not contain such cells, nor is there a significant amount of cell loss in such cultures. In tumors and in spheroids, cells are in 3-dimensional contact, while cells in most other *in vitro* cultures are not. This 3-D contact has been implicated in the radioresistance of cells grown as tumors or spheroids compared to single-cells (7,13,14).

The spheroid system possesses many of the important features of tumors which are lacking in other *in vitro* culture systems. However, the host immunological and hormonal factors (which can complicate the interpretation of *in vivo* experiments) are absent in spheroids. Spheroids can be grown in large quantities in spinner-culture jars. Thus, they have obvious advantages over animal-tumor systems in speed and ease of manipulation as well as expense.

Many cells can be grown as spheroids, including both human and rodent tumors (1,17-19). Recently a method has even been reported for growing spheroids of tumor cells and normal fibroblasts mixed together (22). Spheroids have been used to study hypoxic-cell radiosensitizers (24), penetration of chemotherapeutic compounds (28), and immune mechanisms (26), as weell as in tests of chemotherapeutic drugs (21,27,131).

II. CELL PROLIFERATION KINETICS

A. The Cell Cycle

Central to the study of cell proliferation kinetics is the G_1-S-G_2 model of the intermitotic cell cycle. This model was introduced by Howard and Pelc, based on their autoradiographic studies of the incorporation of ^{32}P into bean root tip cells (29). According to this model, there is a discrete period of pre-mitotic DNA synthesis (S-phase), followed by a 'gap' (G_2) between the end of synthesis and the onset of mitosis. Following mitosis, there is another 'gap' (G_1) before the start of a new round of DNA synthesis. The durations of the phases can be determined by the technique of pulse-labelled mitoses (PLM), which is a refinement of the Howard and Pelc experiments. Cells are 'flash-labelled' for 10 to 30 minutes with tritiated thymidine, which is incorporated only into the DNA of cells in S phase. At intervals thereafter, samples are harvested and prepared for autoradiography. The percent of labelled mitoses is scored for each sample and plotted vs. time after pulse-label. Typically, the resulting curve is like that shown on the next page.

The durations of the phases can be estimated from it empirically or by computer-fitting methods (5). The G_1-S-G_2-Mitosis model of the cell cycle has been confirmed in nearly all eukaryotic systems so far studied. A few notable exceptions have been found; in these cases the cells lack the G_1 phase and begin DNA synthesis immediately following mitosis. In multicellular organisms, a G_1-less cycle has been observed primarily in rapidly dividing systems such as the

cleavage embryos of mouse, sea urchin, and Xenopus, or the myeloid-erythroid series in adult mammals (30). V79 cells in exponential growth have an extremely short (~1 hr) G_1 phase (31), but as the cells become confluent, the G_1 phase lengthens.

In fact, G_1 is the most variable period of the cell cycle. Among individual cells of a homogeneous poulation the length of $S+G_2+M$ is quite constant, but the length of G_1 may vary by as much as a factor of 2 in exponential cell cultures. This variation in G_1 length accounts for most of the variation in T_c among cells of the same population (Prescott, 1976). The mechanism behind this G_1 variability has not been discovered, but it may be related to the observation that _in vivo_ and in certain culture conditions _in vitro_, many cells are subject to a reversible arrest of indeterminate length in G_1 (or a state with G_1 DNA content). This G_1-arrest will be discussed in detail further on.

The G_1-S-G_2 model is simply a description of the pattern of DNA synthesis in the cell cycle, with the two 'gaps' defined as intermitotic periods during which no DNA synthesis is occurring. However, these gaps are not periods of cellular inactivity. During G_1, there is continuous transcriptional activity and accumulation of RNA and proteins: the spectrum of proteins synthesized differs from that seen in S phase or G_2. Similarly, there are biochemical markers for G_2, most notably the synthesis of proteins needed for mitosis (30,32). The existence of cell systems lacking a G_1 phase suggests that either G_1 functions are not required for initiation of S phase

and progress through mitosis, or that these functions can in some situations be performed continuously or in G_2 (30). Taken as a whole, the evidence presented so far suggests that the primary role of G_1 may be in the regulation of the rate of cell proliferation within tissues.

B. Quiescent Cells

Nearly all animal tissues *in vivo* tumors and most normal tissues *in vivo* contain cells which are noncycling (30-34). Noncycling cells can be demonstrated by labelling with tritiated thymidine for a period several times longer than T_c (the individual cell cycle time): unlabelled nuclei are either noncycling or very slowly cycling. In practice, it is difficult to distinguish between these two possibilities. Although slowly cycling cells may differ from noncycling cells in clonogenicity and other properties, for purposes of simplicity I have chosen to lump them together under the terms noncycling or quiescent cells.

Noncycling cells can be divided into several categories depending upon the stage of the cell cycle in which they are arrested and their capacity to re-enter a proliferating state. Some are terminally differentiated and have lost the capacity to divide; these will not be discussed futher as it is unlikely that such cells exist in tumors. Lajtha (34) introduced the term 'G_0' to describe noncycling cells with a G_1 DNa content which retain the capacity to re-enter the proliferating state if given an appropriate stimulus. Re-entry into a cycling state occurs after a delay of 6 to 24 hours between stimulation

and the initiation of DNA synthesis; the duration of this lag depends both upon cell type and stimulus. A classic example of 'G_0' cells is found in rat liver, which can be induced to proliferate by partial hepatectomy (30,32). Another is that of circulating lymphocytes which when treated with a plant lectin such as phytohemagglutinin, cycle for 3 or 4 cell divisions before returning to dormancy (30,32,42).

Cells can become noncycling in the G_2 state, as has been convincingly demonstrated by Gelfant (35) in mouse ear epidermis. There is also evidence that cells may block near the G_1/S boundary--these are distinguished from 'G_0' type cells in that they enter S phase within an hour or two following stimulation (36). Finally, it has been reported that cells can become arrested with S-phase DNA content, however, this is controversial since the studies were performed on tumor cells, which are known to be aneuploid (40). In most systems, quiescent cells in G_2,. S and at the G_1/S border are far outnumbered by those in a G_1-G_0 state. The remainder of this section will focus on quiescent G_1-G_0 type cells.

Some information is available concerning subcellular and biochemical differences between quiescent cells and G_1 cycling cells. Quiescent cells have reduced rates of uptake of many low-molecular-weight nutrients, including phosphate, uridine, hexoses and some amino acids (32,37). However, studies of 3T3 cells showed that changes in phosphate and glucose uptake were not causally related to changes in proliferative status (37). Quiescent cells have lower fluxes of monovalent cations, and the transition to proliferating state is

accompanied by increased activity of the Na^+-K^+ pump (37,38). It is thought that the changes in ion fluxes may relate to hormone action on the cell membrane (38). Noncycling cells have high levels of cyclic AMP compared to proliferating cells (32,37). Ca^{++} and cAMP are implicated in the mechanisms of action of many hormones, and many studies have suggested a significant role for a cAMP in regulation of cell growth in late G_1 (37,38). Recently it was reported that changes in the level of calmodulin (an intracellular Ca^{++} receptor which is involved in the mediation of many of the Ca^{++}-regulated events in eukaryotic cells) correlate strongly with changes from nonproliferative to proliferative states in CHO-K1 cells _in vitro_ (39).

Quiescent lymphocytes have distinctly lower RNA content than G_1 cycling lymphocytes; similar observations have been made for quiescent 3T3 cells _in vitro_ (32,40). Interestingly, G_2-arrested cells also had significantly lower RNA content than their cycling counterparts (40). When quiescent cells are stimulated to proliferate, their rRNA levels increase (40), as does cytoplasmic mRNA (37). Evidence from flow cytometric studies, in which DNA and RNA distributions can be compared in individual cells indicates that cells may have to reach a critical RNA content before entry into S-phase (40). The authors suggest that RNA content may just be a marker of overall metabolic activity. There are differences between the mRNA species found in 'G_0' liver and in regenerating liver. Furthermore, the chromatin of 'G_0' cells appear to be more condensed than that of cycling cells and to have less transcriptional activity (32). These results suggest

that quiescence is associated with changes in gene expression. However, most of the reports of this kind do not compare 'G_0' cells to G_1 cycling cells, but rather compare 'G_0' cells before stimulation to stimulated cells which are progressing toward S-phase or to cycling populations, which contain a mixture of cells.

Theories of G_1 Quiescent Cells. Several hypotheses concerning the nature of G_0 and G_1-quiescent cells exist. Some authors view G_0 as a distinct out-of-cycle phase (32,47). In Baserga's scheme, there is a critical point in mid-G_1 at which cells enter the G_0 state instead of proceeding to the G_1/S boundary (32,41). Temin has proposed a similar model with different terminology (43). This type of model is supported by the evidence cited previously that G_1-quiescent cells have a lower RNA content than G_1-cycling cells. Also consistent with a distinct out-of-cycle G_0 was the finding of Augenlicht and Baserga (41) and others (42) that the longer cells were kept in a quiescent state, the longer the delay before entrance into S-phase. A contrasting view of G_1 quiescent cells is that found in the transition-probability model of Smith and Martin (44). They proposed that as cells reach the critical point in mid-G_1, they have a constant probability per unit time (transition probability) of porgressing past it. Once past this critical point, the cell is committed to completing another mitotic cycle. A decrease in the fraction of proliferating cells would be due to a decreased transition probability--thus, no individual cell would really be considered quiescent.

A third approach is that of Pardee, who used the term "restriction point" and proposed that at this point cells can switch back and forth from a cycling to a noncycling state to cope with varying nutritional conditions, but did not specify the nature of the noncycling state (45). Other possibilities are that cells are simply arrested at a critical point in G_1 for indefinite periods of time, or that some cells are progressing steadily but extremely slowly through G_1 (30,32). All of the models for quiescent cells except the latter share the idea of a critical point partway through G_1, this is because there are markers between this point and the onset of S-phase similar to those observed in cycling cells in late G_1 (32,37).

Quiescent Cells in Tumors and In Vitro. In tumors, noncycling cells are usually concentrated in poorly-vascularized regions, and may be quiescent due to hypoxia, nutritional deficiencies, build-up of metabolic wastes, or a combination of these (3). Dethlefsen (46) suggests that cells which are quiescent because of growth in an unfavorable milieu are not properly termed 'G_0' cells; instead he uses the term 'Q' cells to designate the noncycling population (which may include 'G_0' cells). The noncycling population contains more hypoxic cells (48), and may in some cases have a lower plating efficiency (18) than the proliferating population. However, in some cases Q cells were equal to P cells in plating efficiency (49,50,51); the apparent discrepancy could be due to differences between cell types studied or differences in the method of separation. Separation of

tumor cells on the basis of density shows that the denser cell fractions are enriched for noncycling cells (46,49); however, since an increase in density can be caused by nutrient deprivation, 'Q' fractions obtained by this means may not reflect the properties of tumor 'Q' cells as a whole (46). There is within the P and Q populations themselves considerable heterogeneity with respect to nutritional status, oxygenation, cell size, density, nuclear morphometry, etc. (46). Furthermore, there is probably movement back and forth between the P and Q compartments. Physical migration of cells within tumors has been observed, and shifts between P and Q status may be accompanied by (or result from) such migration.

In vitro cultures of quiescent cells can serve as a model for Q cells in tumors. Such cultures can be obtained in several ways. Normal (untransformed) cell lines such as Chinese hamster HA, human livers LICH, and mouse 3T3 cells reach a plateau in growth after they become confluent, a phenomenon often referred to as 'contact-inhibition' (53-55). Cell number remains constant even though cultures are fed daily, and cells can be held in this 'stationary phase' for a week or more (41,53,54). Most of the cells ($\geq$90 percent) have a G_1 DNA content; they can be stimulated to proliferate by trypsinization and replating at lower density, with a lag of ~12 hr before entering the first S-phase (36,43,53). Plateau phase cells are smaller than exponentially-growing cells, even allowing for the fact that most plateau cells are in G_1 (53). They also have slightly decreased plating efficiency compared to exponential cells (53).

In many plateau-phase studies, cells are grown to confluence without being refed; these cells are certainly nutrient-deprived. Despite this, their kinetic parameters and plating effieincy are similar to those of fed plateau cultures (53). Exponentially growing cells can be rendered quiescent by growth in medium deficient in certain amino acids or having low ($\leq$0.5 percent) serum content (43,45,56-57). The cells are arrested with a G_1 DNA content after 48 to 72 hours; they can be stimulated to proliferate by changing to complete medium.

Multicell spheroids, an in vitro tumor model, develop a subpopulation of noncycling cells once they reach radii $\geq$100-150 μm (approximately the limit of O_2 diffusion in tissue [2,3,11]). Growth in low oxygen tension caused monolayers of Chinese hamster fibroblasts to enter plateau-phase (61,62); the low pO_2 in spheroid cores may be a factor in the development of noncycling cells. Direct electrode measurements of pO_2 in spheroids show that the inner 'Q' cells of spheroids >400 μm are subject to oxygen tensions as low as 0-10 mm Hg (59,60). For comparison, the venous pO_2 in tissues is 20-40 mm (2,11). pH has also been shown to affect cell growth rates, but no data concerning the pH within spheroids is available yet.

The noncycling cells in spheroids are concentrated in the inner regions, and most techniques for separation of P and Q cell fractions rely on this physical localization (18,58,127). Some authors report that inner (presumptive 'Q') cells have lower clonogenicity than outer ('P') cells (18,58); others report equal clonogenicity for Q and P

fractions (46,50). The inner 'Q' cells in spheroids arise under constraints on oxygenation; nutrient supply, and removal of metabolic wastes similar to those in poorly-vascularized tumors. Thus, 'Q' cells in spheroids are probably the best *in vitro* model for 'Q' cells in tumors.

C. Kinetic Parameters of Cell Populations

In discussions of cell populations it is common to use the terms 'cell age' and 'cell age distribution' or 'age structure.' Cell age is measured from the end of mitosis to the point at which the cell divides, dies, or leaves the population (by migration or differentiation). The age distribution is the relationship between cell age and the proportion of cells in a given population, which have that age. Age distribution is usually plotted as the relative probability of finding a cell at age T versus T (5). In growing populations, there are always more young cells than old (5).

The simplest case is that of an exponentially growing population in which all cells are proliferating. The two daughter cells produced at each division are viable and both immediately embark on a new cycle; all cells have the same intermitotic cycle time (T_c). The equation which describes this type of growth is

$$N_t = e^{(bt)}$$

where b = ln2/Tc. This type of population, termed 'type A' by Steel (5), has an age distribution where the probability of finding a

newly-divided cell is exactly twice that of finding a cell just about to divide (e.g. in late (G_2). Mammalian cell cultures *in vitro*, when growing at appropriately low density, are a good example of this.

However, tissues and tumors *in vivo* contain subpopulations of noncycling cells. In this case the age distribution becomes more complex, and the age distributions of proliferating and nonproliferating cells must be considered separately. Cell loss, which is also widespread in *in vivo* populations, adds a further complication. Nonetheless, models of age-distributions can help in interpretation of empirical cell kinetic data. For a more complete discussion of the theory of cell age distributions, see Steel (5).

Growth Fraction. The term 'growth fraction' (abbrev. GF) was introduced by Mendelsohn to describe the fraction of proliferating cells (33); it varies between 0 and 1.0. The exact meaning of the term depends upon the definition (experimental or theoretical) of a proliferating cell (5). Experimentally, there are two methods commonly used to estimate GF. The first uses pulse-labelling with ^{3}H-thymidine and the relationship

$$GF = \frac{L.I.}{(L.I.)_{prolif.}}$$

where L.I. (labelling index) = the fraction of labelled cells in the entire population and $(L.I.)_{prolif.}$ = the fracton of labelled cells in the proliferating subpopulation. If the length of S-phase and of T_c are known (for example, from a labelled-mitosis curve), the

$(L.I.)_{prolif}$ can be estimated as T_S/T_C (greater accuracy can be achieved if mathematical modelling of the PLM data is used [5]). Alternatively, mitotic cells may be taken as representative of proliferating cells. Following the pulse-label, the population is allowed to grow for 3-4 cell cycles. Due to the variability of T_C, the labelled cohort desynchronizes and labelled cells become randomly distributed through the cell cycle. Then, the percentage of labelled mitoses represents the L.I. of the proliferating cells. It should be noted that pulse-label techniques are insensitive to slowly-proliferating subpopulations.

Growth fraction can also be estimated by continuous-labelling techniques. Some authors label for periods much longer than T_C (3-5 times) and take the proportion of labelled cells as the measured GF (21,63). This is based on the assumption that a plateau has been reached where all proliferating cells are labelled and nonproliferating cells are not. As pointed out by Steel (5), this assumption is incorrect and can lead to overestimates of the growth fraction; labelled cells that divide produce labelled daughters, some of which may enter the nonproliferating compartment, but are still counted as proliferating. If a continuous-labelling curve is constructed by sampling at intervals, for an extended period, it would eventually tend to 100 percent labelling. Better estimates can be obtained by extrapolating back to the end of G_2 from the slowly-rising component of continuous-labelling curve, or by use of mathematical modeling (5).

Cell Loss Factor. In addition to having GF < 1 tumor cell populations are also subject to cell loss. This loss can be due to migration of cells out of the tumor, to cell death and to cell maturation (the cell differentiates sufficiently so that it is not recognizable as a tumor cell) (5). The relative proportions of cells lost by each of these mechanisms varies with tumor type. Cell death can be due growth in an unfavorable (e.g., hypoxic, nutrient starved, etc.) environment; death may also occur by the process known as apoptosis, in which isolated cells within otherwise healthy well-nourished regions self-destruct. The cell loss factor ϕ (66) is generally used to quantitate cell loss:

$$\phi = \frac{K_L}{K_P}$$

K_L = rate constant for cell loss; K_p = rate constant for cell production. ϕ can also be expressed

$$\phi = 1 - \frac{T_{potential}}{T_D}$$

If the total cell population is increasing exponentially with a doubling time of T_D. $T_{potential}$ can be calculated if T_c and the growth fraction are known; thus, if T_D is known, ϕ can also be calculated. Alternatively, K_L can be measured directly by monitoring the loss of ^{125}I from tumors labelled with $^{125}IudR$ (67,68). ^{125}I is superior to ^{3}H for this purpose because it is not re-utilized by the surrounding tissue. The process of cell loss can strongly

influence the overall growth rate of a tumor as well as its response to therapeutic regimens.

D. Cell Proliferation in Spheroids

Spheroid growth curves have an initial exponential region which starts to bend over when the spheroid reaches a diameter of about 200 μ (17,63). The growth rate is retarded to a progressively greater degree and may reach a plateau at diameters >1 mm (17). In the region beyond the exponential, spheroid growth (17,19,20) is well described or by a cube-root law similar to that observed for many tumors (5); that is, the cube-root of the volume increases linearly with time. (For a spherical volume like that of a spheroid, the diameter is proportional to the cube-root of the volume; thus, a curve of diameter vs. time which is linear, also represents 'cube-root' growth). Cube-root growth is expected if proliferation is restricted to an external spherical shell (5,20), or if the nutrient supply to the spheroid/tumor is proportional to its surface area (5). A variety of models for spheroid and tumor growth have been proposed, some based on oxygen/nutrient diffusion, some on observations of kinetic parameters such as GF, cell loss, and/or thickness of the dividing layer (20,69-71).

The progressive slowing of spheroid growth rate is not due to a lengthening of Tc, but rather to decreases in growth fraction and increases in cell loss rate. Yuhas and Li have reported that for 300-600 μm spheroids from seven lines of mouse mammary tumors, spheroid doubling time (T_D) correlated with growth fraction, but not with

T_C (19). Durand observed that as V79 spheroids grew from 30 μm to 800 μm, their growth fraction decreased from 0.93 to 0.35 (63). At the same time, the cell loss factor increased from 0.2 to 0.88. Although there was a slight lengthening of T_C, it could not account for the increase in T_D from 10 hr (1-day old spheroids) to 450 hr (25-day old spheroids). These results are in general agreement with results from tumor studies (5,69,72).

Factors associated with the development of quiescent cells (decreasing growth fraction) have already been discussed but not those involved in cell loss. In spheroids, cell loss is due to shedding from the surface as well as to cell death. In some cell lines (notably EMT6) most of the cell loss may be due to shedding (73). The shed cells are >90 percent mitotic and the process may be similar to that in which tissue culture cells 'round up' and detach during mitosis. The rate of shedding depends on spheroid surface area, but not on the stirring speed of suspension cultures (73). Shedding of cells by spheroids may model the first step in metastasis, the shedding of tumor cells into the blood or lymphatic system.

Necrosis develops in the core of spheroids $\geq$400 μm diameter, probably due to hypoxia, nutrient-starvation, build-up of metabolic wastes, or some combination of these (4,59,60). The cells die and disintegrate into simple diffusible materials which eventually move out (65). Cells may also die by apoptosis (a process observed in tumors by Kerr et al [74]), in which the cells first break up into small membrane-bound fragments, then are taken up by neighboring cells.

Apoptosis occurs in isolated cells within otherwise well-nourished regions; it is not restricted to necrotic zones (74). Apoptosis has been implicated as a mode of cell death from radiation on chemical injury, as well as in the regression of tissues during embryogenesis and insect metamorphosis (74).

It is difficult to determine the age of cells being lost. In tumors, there is evidence that cell loss occurs mainly from the oldest nonproliferating subpopulation (5), which would be consistent with death by necrosis. However, there is some evidence indicating that, at least in EMT6 tumors, cells are lost equally from all cell-age categories (67).

Biochemical Factors in Spheroid Growth. The thickness of the viable rim does vary with O_2 tension in the medium (59,75). However, below 5 percent O_2 and above 20 percent O_2 (in the gas phase equilibrated with the medium) varying the O_2 tension does not affect the viable rim (75). Growth in 95 percent O_2 increased the viable rim only a little, and did not change the spheroid growth rate (59). Hypoxic cells in monolayers retain viability for several days (61,62), but hypoxic cells in spheroids die very quickly (76). These results indicate that oxygen is not the critical factor in producing cell necrosis in spheroids. This is supported by electrode measurements showing that necrosis can develop at O_2 tensions (within spheroids) ranging from 0 to 60 mm Hg, depending on growth conditions (60,77).

Glucose concentration plays a role in controlling spheroid growth, particularly under low-oxygen conditions. For V79 spheroids grown at

5 percent O_2, a 3x normal concentration of glucose (3g/l) increased the viable-rim thickness by a small but consistent amount (75). In EMT6/Ro, no necrosis was seen in spheroids grown in 16.5 mM glucose (3g/l) even though the pO_2 in the core was only 3-5mm Hg; whereas spheroids grown in 5.5 mM glucose (normal concentration) and 5 percent O_2, which had a core pO_2 of 57 mm Hg, did develop necrosis (77). Altogether these results suggested that glucose has a significant role in controlling the onset of necrosis. Li, based on studies of monolayer growth rates in different glucose concentrations, suggested that in 9L spheroids the radial depth of the proliferating shell corresponds to the depth at which the glucose level drops below 0.07 mg/ml (78).

Besides oxygen and glucose diffusion, other factors may be at work in causing quiescence and death in inner regions of spheroids. pH can drastically affect the cell population doubling time (79) and also cause cell death (12). Accumulation of wastes such as lactic acid, which is formed by cells wich metabolize glucose under hypoxic conditions (81), is another possibility. Investigation of the effects of lactic acid is currently underway in our laboratory (Hlatky, preliminary data).

III. RADIOBIOLOGY OF MAMMALIAN CELLS

A. Radiation Cell Killing

One of the first applications of ionizing radiation was as a treatment for cancer; its usefulness in this regard is due to its cell-killing effect. It has been established that ionizing radiations kill cells primarily by damaging their DNA (11,82). This damage is dose-dependent and may take the form of single-strand breaks, double-strand breaks, crosslinks, or chemical damage to the base and sugar components. The amount and spectrum of DNA lesions can be affected by a number of environmental factors, including the presence or absence of oxygen during irradiation (11,86). The expression of radiation damage is modified by cellular repair processes (82). These repair processes can restore the DNA to its original condition, but they can also result in incorrect rejoinings, deletions, additions, or substitutions in the original base sequence. Such 'misrepair' can itself lead to cell death or to mutation. Quantitatively, then, the amount of radiation cell killing depends upon both the amount of initial DNA damage and the operation of repair processes (82-84).

The standard assay of radiation cell-killing is the colony-formation assay, which measures the loss of proliferative capacity in irradiated cells. A survival curve is a plot of log surviving fraction vs. dose, and from the shape of this curve inferences can be made about the mechanisms involved in cell killing. For example, the shoulder observed on many survival curves (see diagram) is interpreted as evidence that cells can accumulate sublethal damage up to a critical threshold, beyond which cell death results.

A number of models for radiation survival curves have been developed, which vary in their treatment of both the initial (low-dose) region and the high-dose 'terminal' region of the curve. A complete discussion of survival curves is beyond the scope of this thesis.

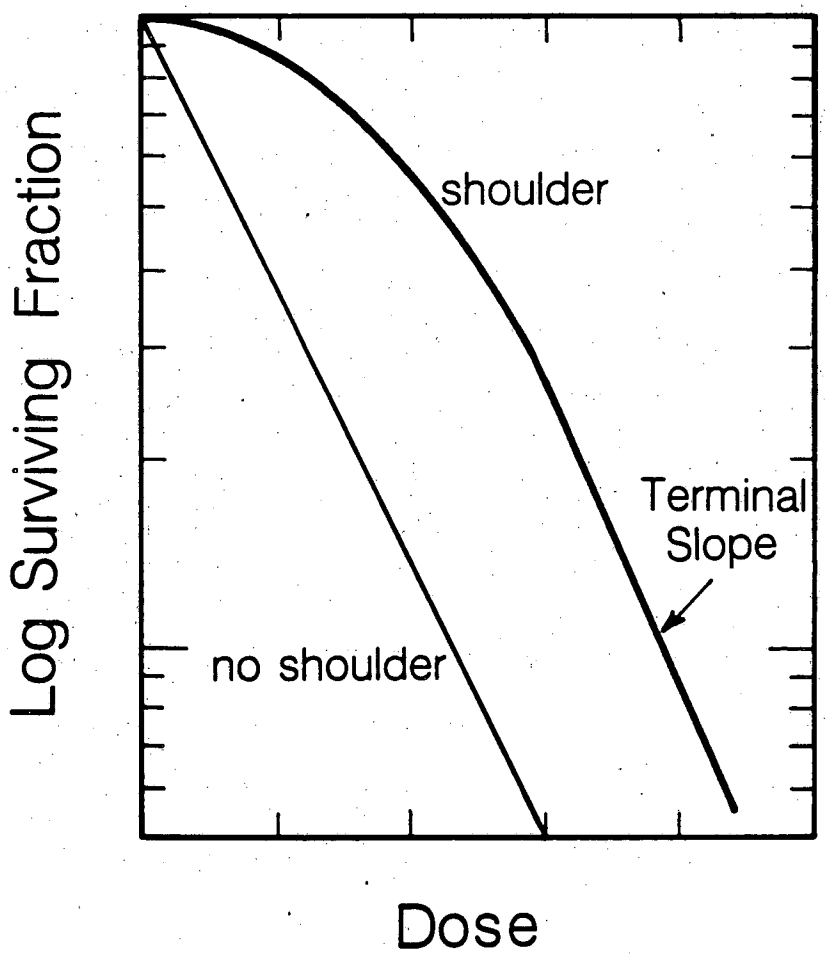

XBL 843-7672

Direct and Indirect Action

Radiation damages cells by 2 general pathways, which are termed 'direct action' and indirect action'. 'Direct action' refers to direct interaction of the ionization event with the target molecule. When ionizations occur in the surrounding (aqueous) cellular medium,

highly-reactive free radicals are formed through interaction with water. These species then attack the target molecule; this is 'indirect action'. The relative proportion of damage occurring by direct and indirect paths depends on the type and quality of the radiation.

The Oxygen Effect. Oxygen acts as a radiosensitizer. The exact mechanism by which oxygen acts is not entirely understood, but it potentiates radiation damage. Oxygen reacts with the free radicals produced by irradiation of the aqueous cellular medium to form longer-lived radical compounds which can themselves damage the cell. Since the original free radicals disappear within about 10^{-5} seconds, oxygen must be present during irradiation to exert its effect.

In terms of biological endpoints, survival curves for hypoxic cells have reduced terminal slopes compared to those for oxic cells. The maximum sensitivity is observed for oxygen tensions above 30 mm Hg; maximum resistance is achieved at zero oxygen tension (11). (By way of comparison, the venous oxygen tension in tissues *in vivo* is typically 20-40 mm Hg [11].) This resistance is quantified by the oxygen enhancement ratio (OER), defined as the ratio of doses required to produce the same survival under hypoxic and aerobic conditons. Maximal OER values for mammalian cells are about 3 (11,95). The oxygen effect is of importance in clinical radiotherapy: many human tumors contain a fraction of resistant hypoxic cells. These hypoxic cells are thought to account for the difficulty of eradication of some

tumors by X-irradiation; following a dose which kills the oxic cells, many hypoxic cells survive, are reoxygenated and can proliferate so that the tumor regrows (2).

Radiation Quality. The spectrum of lesions and the biological effect produced by a given dose of ionizing radiation can vary greatly among different types of radiation. Linear energy transfer (LET) is the quantity often used to compare different radiations: it is defined as the amount of energy deposited (through ionizations and excitations) per unit length along the track of an ionizing particle. Photon radiations such as cobalt-60 γ-rays or 250 kvp x-rays have a rather sparse pattern of ionizations, and are considered low-LET radiations. They cause damage primarily through the pathway of indirect action; thus the amount of damage depends also on whether oxygen is present. Heavy charged particles, on the other hand, produce tracks of densely clustered ionizations, and may have LET values up to 1000 times those of γ-rays. Such densely-ionizing radiations cause damage primarily through 'direct action', which is insensitive to the presence of oxygen. Thus, high-LET radiations can be used in clinical radiotherapy to circumvent the radioprotective effect of hypoxia in tumors.

High-LET radiations are also more effective in cell killing per unit dose than low-LET radiations. The relative biological effectiveness (RBE) of a given radiation is defined with respect to a standard, 250 kvp x-rays. RBE is the ratio of doses of standard and test radiation which yield the same biological effect. Survival

curves for high-LET radiations have a much-reduced or absent shoulder as compared to low-LET survival curves, implying that damage produced by high-LET radiation is not repairable. Because of this difference in shoulder between low- and high-LET radiation, the RBE varies with dose and is greatest in the low-dose region (unlike the OER). Thus, the fractionated treatment schedules used by radiotherapists may offer even greater therapeutic advantages with high-LET radiation.

Repair of Radiation Damage. As previously mentioned, the shoulder observed on most x-ray survival curves has been interpreted as evidence that cells can accumulate sublethal damage (SLD). Since by definition 'sublethal' damage does not cause cell death, it is only detectable by split-dose experiments like those pioneered by Elkind and Sutton (85). If a given total dose of radiation is administered in two fractions separated by an interval of tens of minutes or more, cell survival is higher than if the same total dose is given at once. This result demonstrates that cells given the split-dose regimen were able to repair sublethal damage from the first fraction before it could interact with damage from the second fraction (11,85,86). Repair of sublethal damage does not change the shape of the survival curve. If cells which have been given an initial dose in the shoulder region of the survival curve are allowed to repair all sublethal damage, then given the second exposure to graded doses of radiation, the shape of this survival curve (including both the slope and the shoulder) is the same as for a single-dose 'normal' survival curve.

A second type of repair occurs when, under special post-irradiation conditions, cells can repair damage which would ordinarily lead to cell death. This is called 'potentially-lethal damage' (PLD) repair. In most *in vitro* survival assays, exponentially growing cells are irradiated, then immediately trypsinized and seeded for colony-formation. If instead the cells are irradiated and then held in a stationary state for up to 24 hrs before trypsinization, cell survival is increased over that resulting from immediate trypsinization. Thus, post-irradiation holding allowed cells to repair potentially lethal damage (PLD) injury which otherwise would cause cell death. The cells are held in a stationary phase as confluent (and quiescent) monolayers, so the measured increase in survival is not due to any effects of proliferation within the population. If a complete survival curve is done under conditions allowing maximum PLD repair, the slope is found to be decreased over that for a 'normal' (no post-irradiation holding) survival curve.

Both SLD repair and PLD repair have been demonstrated *in vivo* as well as *in vitro* (11). SLD repair is thought to account for most of the sparing effect on normal tissues of the multiple-fraction treatment schedules commonly used in clinical radiotherapy (11). The mechanisms for SLD and PLD repair have not yet been elucidated, nor have the two types of damage been correlated with any specific radiation-induced DNA lesions.

Cell Age Response. It has been well-established that radiosensitivity varies through the cell cycle (86). The pattern varies somewhat among different cell lines, but in general is as follows: late-S is the most resistant phase and mitosis is the most sensitive. Cells with a long G_1 period may have a peak of intermediate resistance in late G_1 (85). The magnitude of the difference in survival depends upon cell line; in V79 cells it is about a factor of 7 (85,86), while 9L cells show almost no variation of radiosensitivity with cell age (93,94). Radiotherapists use multiple-dose schedules. Irradiation induces a partial synchrony in the surviving cells; with correct timing between doses the killing of tumor cells can be maximized (11,86). This partial synchrony is due to the preferential survival after the first dose of cells in the most resistant phase of the cycle as well as to the effects of radiation-induced G_2-delay.

B. Radiation-Induced Division Delay

Understanding of the radiation-induced division delay (RIDD) kinetics combined with the cell-age dependence of radiosensitivity is important in the optimization of multi-fraction treatment schedules. Irradiated cells are reversibly blocked in mid-G_2 (11,97-101). This is observed as a drastic drop in mitotic index followed by recovery to normal levels, as a lengthening of the time it takes labelled cells (labelled just before or during irradiation) to reach mitosis, or by flow cytometry as a piling-up of cells in G_2. The length of the delay is dose-dependent and cell-age dependent, typically about 30 min

to 1 hr. per 100 rads of x-rays in cells that were in G_2 at irradiation (100,101). Cells in G_1 and S are delayed less than G_2 cells, thus they may 'catch up' with G_2 cells. The G_2 delay is strictly transient, and once irradiated cells have passed through mitosis their cycle returns to normal (97,98). The lesion(s) causing radiation-induced division delay appear to be distinct from those involved in cell killing; however, the target is in the nucleus (102-106). There is some evidence suggesting that the nuclear membrane is involved (103), but most recent studies point to DNA as the target (103,104-106). Radiation also exerts a transient effect on entry into S phase and the duration of S, but to a much smaller degree than for G_2 (92,108). High-LET radiations produce a much longer G_2-delay than x-rays (per unit dose).

C. Radiation Response of Spheroids

For many cell lines, survival is greater if cells are irradiated as spheroids than if they are irradiated as exponentially-growing monolayers (4,15,21). It is not due to a difference in the amount of initial DNA damage measured as single-strand breaks between spheroids and monolayers (109-110). Spheroid cells are in 3-dimensional cell-cell contact and this plays a significant role in spheroid radioresistance (13,15,111). In addition, spheroid survival curves reflect the effects of cell-cycle redistribution and hypoxia, and may be multiphasic (4,112). As cell-age distribution and fraction of hypoxic cells vary with the size of the spheriods, so do spheroid survival curves.

Cell-Cell Contact. Growth and irradiation as multicell spheroids has been shown to enhance radioresistance of many cell types; this has been termed contact-effect. In V79 cells contact-effect has been demonstrated in very small (30-60 μm diameter) spheroids, in which the potential complications of hypoxia and cell-cycle redistribution are eliminated (111). In many cases, the resistance appears as an increased shoulder on the survival curve (111,113), which according to traditional interpretation indicates an increased ability to sustain and repair sublethal damage. In some cases, including 9L, the shoulder is not affected but the terminal slope is decreased (15,21). Contact-effect has also been demonstrated in rodent tumors *in vivo* (7,96,114) and in human tumor xenografts (16).

Experiments in which spheroids are dissociated at various intervals prior to irradiation and plating show that there is also a residual contact-effect (4,14,111). The contact-effect resistance decays over a period of one T_c or less, back to the sensitivity of monolayer cells (4,111). V79 (111) and other, spheroid cells (15) demonstrate some residual effect, as do KHT tumors *in vivo* (7); however, cells from human tumor xenografts did not (16). In KHT tumor cells, the contact-effect did not decay if cells were held at 4°C (instead of 22° or 37°) between dissociation and irradiation, implying that metabolic processes were involved (7). However, if intact V79 spheroids were incubated at 4°C for 20 minutes prior to irradiation, the protection of the contact-effect was eliminated (115).

The mechanism of contact-effect is not yet known, but it has been speculated that gap-junctions are involved (15). Gap junctions allow the passage of molecules of up to 1000-2000 daltons which, however, probably excludes any DNA repair enzymes (116-118). A commonly-used indicator for the presence of gap-junctions is the degree of ionic coupling, measured as intercellular impedance. The degree to which a given cell line shows contact-effect in spheroids appears to correlate with the degree of ionic coupling present in its monolayer cultures (15). However, when coupling was measured in the outer layers of 300 μm spheroids, it was found to be lower than in monolayers and to decrease further as the spheroid increased in size (14).

A 'feeder-cell effect', which may be related to the contact effect, has been observed in the 9L cell line (119). Survival levels of cells from 9L monolayers are strongly dependent on the feeder-cells (total cell number/dish) below about 5×10^4 cells/25 cm^2 flask, with a plateau in survival between 5×10^4 and 1×10^5 cells/flask. Cells grown as spheroids have the same survival regardless of total cell number (below 10^5/dish). Thus, growth as a spheroid can apparently substitute for the survival-enhancing affects of feeder cells.

Hypoxic Cells in Spheroids. Once the spheroid reaches a diameter of 300 μm or more, cells in the core may become hypoxic due to competition between O_2 diffusion and O_2 consumption by the outer cell layers (126). As previously mentioned, hypoxic cells are quite radioresistant compared to oxic cells. Presence of a radiobiologically

hypoxic subpopulation is indicated by a 'tail' of decreased slope on the survival curve; the fraction of hypoxic cells can be estimated by extrapolating the 'tail' back to the y-axis. Although the presence of fully (radiobiologically) hypoxic cells in tumors is well-documented (6,11,96), the situtation in spheroids is less clear-cut. 600 μm V79 spheroids had an anoxic fraction of 5-7 percent, but larger spheroids contained fewer hypoxic cells (112). In this and other studies, the terminal slope of the hypoxic-cell region of the survival curve is intermediate between that for fully-oxic and fully hypoxic cells (50,120). Based on the observation that hypoxic cells in spheroids die very quickly, it has been suggested that the inner cells in some spheroid types may die before reaching full radiobiological hypoxia (76). Recently, Durand (121) used a cell-sorting technique to demonstrate that the OER was the same in all regions of spheroids. Another recent study showed that the apparent absence of fully hypoxic cells in spheroids may be an artefact caused by growing spheroids at high density, then transferring to low density before irradiation (122). The authors also showed that if spheroid density is properly controlled, EMT6 spheroids do contain anoxic cells having the same radiosensitivity as anoxic cells in EMT6 tumors. Some spheroids may genuinely lack hypoxic cells. 9L spheroids had <3 percent detectable hypoxic cells (21,119). This observation is supported by evidence that 9L tumors *in vivo* also lack a hypoxic fraction (114,123). Spheroid radiobiological response (and especially the detection of hypoxic cells) is strongly influenced by irradiation conditions such

as temperature, whether the culture is stirred and culture density, as well as by dissociation technique (112). Particular care is necessary in the planning and interpretation of spheroid radiation survival experiments.

Cell-Cycle Effects in Spheroids. For V79 cells, the age-response of cells in spheroids is qualitatively similar to that of monolayer cells, but the spheroid cells are more resistant in each phase than their monolayer counterparts (4,125). Since S-phase is by far the most resistant, as cells begin to shift into G_0/G_1 (at a spheroid diameter of about 150 μm) the radioresistance of the spheroid as a whole actually decreases compared to that of smaller spheroids (125). No such comparison of spheroid vs. monolayer cell-age response has been reported for other cell lines. Shifting of cells out of S phase may be less important in a cell line such as 9L, which shows little variation in radiosensitivity with cell age in monolayer cultures (93,94). As spheroids mature, they develop regions of quiescent cells. A possibility which has not been ruled out is that 'G_0' cells are more radioresistant than G_1 cells. It has been suggested that quiescent cells in tumors may be radioresistant, accounting for the difficulty of sterilizing them by irradiation (2,11).

It has been reported that spheroid cells are less susceptible to radiation-induced division delay than monolayer cells (128,129). If this is also true of tumor cells, it would have significance for the planning of radiotherapy protocols.

IV. RATIONALE

Clinically, tumors of glial origin are highly malignant and difficult to treat successfully by conventional techniques. The 9L rat gliosarcoma was developed as an *in vivo-in vitro* model of such tumors, in order to better study their properties and to search for more effective treatment modes (124). Since the spheroid culture method offers advantages of simplicity and speed, while retaining many of the properties of *in vivo* tumors, which are lost in monolayer cultures, it was a natural step to culture 9L cells as spheroids. This was first done by Deen et al. (21) and the technique adapted for use in our laboratory, by Rodriguez and Alpen (119,130). 9L spheroids are being used to study the effects of anti-tumor drugs (21,131) and radiation, including heavy ions (130). Since spheroid properties can vary significantly among different culture conditions (60,112), cell lines (4,15,21,73), and even among different sublines (112), each spheroid system needs to be characterized individually.

As has been found for many other spheroid systems, 9L cells irradiated as spheroids are more radioresistant than 9L cells irradiated as monolayers (21). The reasons for this are not yet understood. Since one major difference between monolayer and spheroid cultures is in their cell population kinetics, I decided to try to evaluate their influence on the radiation response of spheroids. One possibility was that quiescent or 'G_0' cells were more radioresistant than cycling cells. 9L spheroids as well as tumors *in vivo* contain very few (<3 percent) hypoxic cells (21,114,130); also, 9L cells have

a very flat age-response to radiation (93,94), so it is possible to study the radiation response of G_1-quiescent cells without the complicating factors of radiobiological hypoxia and variations in radiosensitivity through the cell cycle. One approach would have been to use fractionated dissociation techniques to separate the outer layer of cycling cells from the core of noncycling cells, then to plate those fractions separately for colony formation. This method assumes that all cycling cells are confined to the outer layer and all noncycling cells to the inner region; we know that this is an over-simplification. Mitotic figures have been observed quite deep in spheroid cross-sections (59) and the labelling index (indicating proportion of S-phase cells) in the outer layers of spheroids may be as little as 60 percent of that seen in an exponential growing monolayer (where all cells are cycling) (18). Instead, I modified the 'suicide' technique, originally used to investigate the cell age-response to radiation, in which cells are treated with high-specific-activity tritiated thymidine to kill S-phase cells (132). I extended the period of treatment so that only quiescent or very slowly cycling cells would escape the incorporation of ^{3}H-thymidine. Then, the survival of these quiescent cells could be compared to the radioresponse of the entire spheroid cell population.

If G_1-quiescent cells are more resistant than cycling cells, one would expect larger spheroids with greater proportions of such cells to be more radioresistant than smaller spheroids. However, 9L spheroids ranging from 150 μm to 500 μm in diameter do not differ in

radiosensitivity (130). An alternate explanation is that the rate of cell loss is much higher in large spheroids than in small ones, resulting in similar proportions of G_1-quiescent cells for spheroids of varying sizes. Cell loss rate can be measured using ^{125}IUdR or calculated from a knowledge of other cell kinetic parameters. I chose the latter approach since it was also of interest to correlate the contributions of various cell kinetic parameters with the overall growth rates of spheroids at different stages. The region of growth from 5-10 cells aggregates to diameter of ~1 mm may resemble the early stages of metastatic foci. Such early stages cannot be studied *in vivo* by present methods; information from spheroid systems may have valuable applications to cancer treatment. Therefore, I measured T_c, growth fraction, T_D (doubling-time of the spheroid cell number), and used these figures to calculate the cell loss factor. In addition, I measured cell shedding, a component of the total cell loss.

Finally, I also compared the length of radiation-induced division delay in spheroids and monolayers. It has been reported for V79 cells that RIDD is less in spheroids than in monolayers (128,129). This conclusion was based on flow cytofluorimetry (FMF) data. The FMF technique yields a histogram of the DNA content of a cell population; it may be insensitive to changes in a population which contains a large proportion of quiescent cells (which have a G_1 DNA content). So I decided to use the technique of pulse-labelled mitoses, which directly measures the movement of cycling cells (specifically, S-phase cells) through the cell cycle.

MATERIALS AND METHODS

A. 9L Cells and Stock Cultures

All experiments were performed on 9L rat brain tumor cells. The 9L cell line, a mixed gliosarcoma, orginated as an N-nitrosomethylurea-induced tumor in a CD Fischer rat. The tumor was then developed as an *in vivo-in vitro* brain tumor model (124), and is now in use in several laboratories around the country. Our initial stock of cells was obtained from Dennis Deen of the Brain Tumor Research Center, Univ. of California School of Medicine, San Francisco. 9L cells may be grown either *in vivo* as a solid tumor or *in vitro* as a monolayer, single-cell suspension or as spheroids. Most experiments described herein were done on spheroid cultures.

Stock cultures were maintained as monolayers in 75 cm^2 flasks to provide cells for the initiation of spheroid cultures. Since it is believed that over long periods of *in vitro* culture the 9L cells may undergo changes, including loss of tumorigenicity, stock cultures were renewed from early-passage frozen stocks every 3 months. Culture medium for both monolayers and spheroids consisted of Eagle's MEM with Earle's Salts (Gibco, made from autoclavable powder) supplemented with 12.5 percent newborn calf serum (heat-inactivated), 2.5 percent fetal calf serum, and glutamine. Spheroid culture medium contained gentamicin. Monolayers were maintained in exponential growth by sub-culturing twice a week, seeding two flasks: one in medium with antibiotic and one in medium without antibiotic. Monolayers were kept in incubators at 37°C with a humidified 5 percent CO_2 atmosphere. Monolayer stock cultures were periodically tested for mycoplasma.

B. Spheroid Culture

Spheroids were initiated by seeding 7.5 x 10^5 cells/dish into 12 ml of medium in Integrid bacteriological plastic dishes. Few cells attach to these dishes; most remain in suspension and form small aggregates within a day or two. After one to two days' incubation, the contents of four dishes were filtered through 50 μm or 100 μm nylon mesh, to remove outsize and branching clumps, and the filtrate transferred to a spinner jar (Bellco, Inc.) with 100 ml fresh medium (totally 150 ml of spheroid suspension per jar). The spinner jars ware kept in an Incucover at 37°C, with magnetic stirring, and were gassed continuously with a humidified 5 percent CO_2-95 percent air mixture. Beginning two days after transfer to the spinner jar, the spheroids were fed daily. The spheroids are allowed to settle out of the medium, 125 ml of the medium is aspirated, and 125 ml of fresh pre-warmed medium is replaced. This feeding technique removes most of the shed cells, to prevent small new spheroids from developing. Preliminary experiments indicated that at spheroid diameters greater than 400 μm, spheroid growth rate was influenced by culture density. Therefore, at each feeding the number of spheroids per jar was reduced, to ensure that the culture density never exceeded 2.5 x 10^5 cells/ml.

Spheroid Sizing. Spheroid diameters were measured on a Zeiss Opton inverted phase microscope with objectives containing calibrated reticules. Two orthogonal measurements were taken of each spheroid and the spheroid diameter calculated as $(d_1 d_2)^{1/2}$. Spheroid

cultures had CV's ranging from 8 percent to 16 percent, averaging around 11 percent (n = 30). Samples of spheroids for various experiments were selected by eye using a Pasteur pipette and checked under the microscope for accurate sizing.

In some cases, spheroid populations were sorted using a spheroid separator modeled after the one described by Wigle, Freyer, and Sutherland (80). Basically it is a lg sedimentation column, with layers of precision-woven nylon mesh (Tetko, Inc.) which can be varied to select a population of the desired size. However, due to the somewhat elliptical shape of many 9L spheroids, separations achieved by this means still had CV's of 7 to 9 percent. Particularly for experiments involving larger spheroids, where fewer spheroids were needed to yield a sufficient number of cells, the by-hand selection technique proved simpler and more accurate.

Dissociation of Spheroids. Type IX neutral protease (Sigma) was used for dissociation of spheroids to single cells. Type IX protease has been found to give superior cell yield and viability in dissociations of tumors (154). The working solution consisted of 10 mg/ml protease in spinner-MEM (Earle's salts, modified for suspension culture, Gibco) supplemented with 5 percent calf serum. Working solution was prepared from frozen concentrate no more than one day in advance of use, and kept refrigerated or on ice at all times except during spheroid dissociations. All incubations of spheroids with protease were done at 37°C.

Dissociation procedures varied somewhat with the size of the spheroid, but all involved a pre-treatment with EBSS-EDTA (Earle's Basic Saline Solution w/o Ca^+ and Mg^+, Gibco; with .002 g/l EDTA added) at room temperature, followed by incubation in 10 mg/ml protease at 37°C. For spheroids less than 300 μm diameter, 300 to 1100 spheroids were pelleted (5 minutes at 1000 rpm). The medium was aspirated and the spheroids resuspended in 5 ml of EBSS-EDTA for 5 minutes. The spheroids were pelleted again, the EBSS-EDTA aspirated, and the spheroids resuspended in 2 to 10 ml protease solution. The spheroids were then incubated at 37°C, with vortexing at 5 minute interals, until fully dissociated (5 to 15 minutes). For larger spheroids, larger quantities of EBSS-EDTA and protease and longer incubation times were required. All cell suspensions prepared from spheroids were examined microscopically to ensure that spheroids were indeed fully dissociated with no remaining 'cores' of undissociated cells.

Spheroid Growth Rates. Spheroid growth rates were determined by daily measurement of the number of cells per spheroid in a culture as it grows from an average diameter of 80 μm to over 900 μm (about 25 days). For each measurement, a representative sample of spheroids was removed and deposited in drops of about 0.1 ml on plastic culture dish. Under the microscope, the total number of spheroids in the sample was counted; the first forty were sized. The entire sample was then dissociated to single cells, a portion counted on the Coulter

Counter, and the number of cells per spheroid was calculated. The number of spheroids per sample ranged from 100 (for spheroids 750 μm) to as many as 1000 (for 80 μm spheroids).

Cell Shedding. A known quantity of spheroids was rinsed thoroughly to remove any loose cells, then transferred to a clean, siliconized spinner jar with fresh medium. Part of the sample was sized under the microscope. The spheroids were placed in the incubator under usual growth conditions. After an interval of 2 to 4 hours, the spheroids were allowed to settle out and 90 percent of the medium was removed. Fresh medium was added back to the jar, and after a second incubation interval, the medium was again removed.

The samples were pelleted for 20 minutes at 1000 rpm in 50 ml centrifuge tubes (Corning). The medium was aspirated with care not to disturb the pellet. Although the shed cells were primarily singlets, the pelleting process resulted in some aggregation. The pellet was therefore dissociated using EBSS-EDTA and protease. An aliquot was counted, and the number of cells shed per spheroid per hour was calculated for each collection interval. The total number of shed cells per interval was typically 1-2 x 10^5.

C. Tritium-Labelling Experiments

Several types of experiments were done using tritiated thymidine (^{3}H-TdR) to label or kill DNA-synthesizing cells.

Pulse-labelled Mitosis Curves: monolayers: 48 hours before labelling, T-25 culture flasks (Falcon) were seeded with 1 x 10^5 cells each. Media was removed from the flasks, pooled in a sterile

jar and kept at 37°C. 2 ml of prewarmed medium containing 1 μCi/ml ^{3}H-TdR (6.7 Ci/mmol, New England Nuclear) was added to each flask, and the flasks were incubated at 37°C for 15 minutes. The labelling medium was then removed, and the monolayers were rinsed twice with EBSS. 5 ml of the reserved original medium was replaced in each flask, and the flasks were returned to the incubator. At one to two hour intervals thereafter, flasks of cells were trypsinized to single-cell suspensions, fixed in Carnoy's (3:1 methanol-acetic acid) and dropped on slides for subsequent autoradiography. For some experiments, the flasks of cells were irradiated after the pulse-label had been washed out. Flasks were irradiated in groups of four at room temperature, then placed on ice until all irradiations were completed. All flasks were then returned to the incubator and later harvested as above. A trial experiment indicated that holding at room temperature or below caused a block in cell progression, which was reversed with no perturbing effects as soon as the cells were returned to 37°C.

Spheroid cultures were pulse-labelled by adding ^{3}H-TdR (6.7 Ci/mmole, NEN) spinner jar to the final concentration of 1 μCi/ml. Cultures were labelled for 30 minutes to allow sufficient penetration into the center of the spheroid. The spheroids were then transferred from the labelling jar to a test tube and rinsed 3 times with EBSS. The rinsed spheroids were placed in a clean jar in pre-equilibrated fresh medium. Samples were removed at intervals, reduced to single-cell suspension, fixed in Carnoy's and dropped on sides as for monolayers. In some cases, the spheroids were irradiated after the

label was washed out. The spheroids were put in a T-25 flask with 1-2 ml fresh medium and irradiated at room temperature. They were put on ice immediately after irradiation and kept there until they could be transferred to a pre-equilibrated clean spinner jar. A control experiment in which the spheroids were labelled in fresh medium and then replaced in the original ("conditioned") growth medium (as was done with the monolayers) indicated that this did not alter the results.

Two slides per sample were dipped in Kodak NTB 2 emulsion at 42°C. The slides were air-dried, then transferred to light-tight boxes containing desiccant capsules and exposed at 4°C. Exposure times were determined by trial and error: monolayer PLM slides were exposed for 1 day, spheroid PLM slides for 3 days. The slides were developed for 6 minutes in Kodak D-170 developer, fixed and stained with 5 percent Giemsa for 10 to 15 minutes. 100 mitoses per point were scored (except in a few instances where the mitotic yield was too low, in which case 50 mitoses were counted). Mitoses with >10 grains were scored as labelled.

The threshold of 10 grains/mitosis was chosen because it yielded the best and most reproducible results for both spheroid and monolayer experiments. As shown by Shackney et al. (153) the choice of appropriate threshold varies according to exposure time, so that basically the same PLM result is obtained for a variety of combinations of threshold and exposure time. Curves obtained with low counting thresholds, where the signal-to-noise ratio is lowest, are much more subject to random fluctuations (144,153).

Continuous-Labelling Experiments: this technique was used to measure the growth fraction in spheroids of varying sizes. To a spinner jar containing spheroids and growth medium, ^{3}H-TdR (6.7 Ci/mmole) was added to a concentration of 0.1 μCi/ml. To prevent significant depletion of label over periods of 12 or more hours, unlabelled thymidine was added sufficient to make the total (labelled + unlabelled) thymidine concentration 2.5×10^{-6} M with a final specific activity of 42 mCi/mmole. After 12 hours, a sample of spheroids was removed, dissociated and prepared for autoradiography as previously described. A baseline experiment was also performed in which samples were harvested at suitable intervals up to 22 hours. Autoradiography was done as described earlier, and slides were exposed for 3 days. Background was <1 grain per cell, so a cell was scored as 'labelled' if it had >5 grains. 1000 cells were scored per sample.

Suicide-Labelling Experiments: The term 'suicide'-treatment as used here refers to the killing of cells through uptake of high-specific-activity ^{3}H-thymidine. Sufficient uptake of ^{3}H-thymidine into the nucleus results in killing of the cell by radiation toxicity of the tritium. Only cells in S-phase incorporate ^{3}H-thymidine into the nucleus; since the range of the ^{3}H beta-ray is quite short, the tritium must essentially be in the nucleus in order to cause cell killing (132). In the spheroid, then, only cells which passed through S-phase during the treatment with ^{3}H-thymidine would be killed.

In these experiments, approximately 200 spheroids of diameter 800 μm were placed in 100 ml medium in a spinner jar and treated with 100 μCi of ^{3}H-TdR (20 Ci/mmole, NEN) for 16 hours. After the first ten hours, the label in the medium was replenished. 80 ml of medium was removed from the jar and discarded, then replaced with 80 ml of fresh pre-warmed medium and 80 μCi ^{3}H-TdR. At the end of treatment, the spheroids were transferred to a test tube and rinsed three times with EBSS. The spheroids were then divided into groups of 10 and placed in the center wells of 24-well cluster plates (Costar , Cambridge, Ma) in 1 ml medium per well. Alternate marked wells in each dish contained untreated control spheroids (these were 'siblings' of the treated spheroids: both came from the same initial batch of spheroids, which had been split two or three days prior to the experiment). The spheroids were irradiated in the dishes, then immediately transferred to test tubes and kept on ice until dissociation. Control and suicide-treated spheroids were dissociated in parallel to single-cell suspension, then counted, diluted and seeded for colony formation in 25 cm^2 flasks.

D. Colony Formation Assay

All colony formation assays were carried out using feeder cells: one day in advance, flasks were seeded with heavily-irradiated 9L cells. The number of feeder cells was adjusted as as to give a total number (feeder + test cells) of 7.5 x 10^4 cells per 25 cm^2 flasks; this number of feeder cells was previously found to be in the optimal range for CFE in 9L cells (119). For each sample, two dilutions of

test cells were seeded (five replicates per sample dilution) so as to yield 100 colonies and 50 colonies per flask, respectively. The flasks were incubated at 37°C for nine to eleven days depending upon radiation dose. They were then stained with methylene blue, air-dried and counted. The criterion for counting was 50 cells/colony, <1/3 giant cells.

E. Irradiations

All irradiations were carried out using a 150 kVp Phillips x-ray machine, with 1 mm Al and 0.5 mm Cu filtration. Dosimetry was done with a Victoreen r-meter. All irradiations were done at room temperature, and cells were placed on ice immediately afterward. Two irradiation geometries were used. For the suicide experiments, all spheroids were in the center wells of Costar 24-well plates. The plates were on a rotating platform 9 cm below the aperture. The dose rate was over 200 rad/min, with no measurable variation across the diameter of the wells.

For the studies of radiation-induced mitotic delay, the technique of pulse-labelled mitoses used on monolayers necessitated a different set-up. 25 cm^2 flasks containing the pulse-labelled monolayers were irradiated in groups of four, arranged in an open square on the rotating platform, 25 um below the aperture. The dose-rate was 50 to 60 rad/min, and varied by as much as 4 rad/min between the outer and inner edges of the flask.

RESULTS

I. SPHEROID GROWTH KINETICS

A. Spheroid Growth Rates

Figure 1 shows spheroid growth curves, measured as the number of cells per spheroid, beginning 1 day after transfer from agar dishes to spinner jars. The growth curves were measured under two growth conditions in parallel cultures. In one flask, the cell density was kept around 1.5×10^5 cells/ml medium and never allowed to exceed 2.5×10^5 cells per ml; in the sibling culture, cell density was not controlled, increasing to over 10^6 cells/ml as the spheroids grew beyond 400 μm in diameter. Looking first at the controlled-density curve, it can be seen that in the early region (spheroid diameters from 80–200 μm approx.) spheroid growth fits on exponential with a doubling time of about 19 hours. This doubling time is only a little longer than the monolayer doubling time of 16 hrs. (data not shown). Beyond about 4 days (200 μm diameter), the doubling-time increases sharply and no longer fits an exponential; rather, the curve is now continuously bending. Doubling-times in the continuously-bending portion were obtained by estimating tangents to the curve at points corresponding to various spheroid sizes. Between 250 μm and 500 μm diameter (from day 5 to day 13 approximately), the T_D increases by a factor of 2, from 28 hr to 54 hr. Beyond 600 μm, the doubling-time increases sharply to ~90 hours at 700 μm, then more gradually to 110 hours at 800 μm and 139 hr at 1000 μm. The growth curve can be roughly divided into three regions: the early exponential region, a

'middle' region between 200 and 600 μm diameter, and a 'late' region beyond 600 μm. Although the distinction between the 'middle' and 'late' regions of the growth curve may seem arbitrary, it is supported by the data on T_c, growth fraction, and cell loss factor ϕ.

Looking at the growth curve for spheroids growing under conditions of uncontrolled, high density, it can be seen that the early and middle regions are essentially the same as for the density-controlled cultures. However, the high-density cultures entered the 'late' growth region several days sooner than the low-density spheroids, just beyond 400 μm in diameter. The 'late' region of growth for the two culture conditions is essentially the same except for the earlier onset in the high-density cultures. All cultures were started from the same number of cells; initial densities (1-2 days of culture) were typically 2-4 x 10^4 cells/ml. In the density-controlled cultures, removal of spheroids (to keep the cell number per ml at ~1.5 x 10^5) began after about 1 week in culture (d ~250μm). In the uncontrolled cultures, cell density generally exceeded 10^6 cells/ml by about ten days (d ~350 μm). After that it generally stayed in that range, due to the daily removal of samples (data not shown). For spheroids grown at high density the shift into the 'late' region occurred about four days after the density exceeded 2.5 x 10^5 cells/ml.

Figures 2a and 3b display the increase in spheroid diameter vs. time and the number of cells per spheroid vs. spheroid volume, respectively. As can be seen, spheroid diameter increases linearly beyond about 300 μm diameter. The number of cells per spheroid was

plotted vs. spheroid volume for two reasons: first, to give an idea of the reproducibility of the cell number and volume measurements, and second, to see if anything could be learned about cell packing in spheroids as they matured. For spheroids between 200 and 800 μm the plot is linear. Below 200 μm and about 800 μm, the plot deviates from the central linear portion. In the region above 800 μm the total number of spheroids per jar is now ~100-150, so samples must be limited to about 50 spheroids; thus, the data points in this region are subject to somewhat larger sampling errors.

B. Cell Cycle Parameters

Figure 3 displays pulse-labelled mitoses curve for 9L monolayers, 400 μm and 800 μm spheroids. It is immediately obvious that there is a significant increase in T_c of 9L spheroids over that of monolayers. Monolayers have a T_c of about 16.6 hours, with G_2 + 1/2 M of approx. 2.3 hr, S ~9.4 hr, and G_1 ~4.5-5 hr. T_c of spheroids is 24 hours for 400 μm and 28 hr at 800 μm, an increase of nearly 70 percent. G_2 and S phase are nearly unchanged; all of the lengthening is in the G_1 portion of the cycle. Since the doubling-time of very small spheroids is 19 hr (Fig. 1) the T_c of such spheroids cannot be more than 19 h and it is likely to be the same as in monolayer. Over 1/2 of the increase in T_c takes place during a period of about five days, from 200 to 400 μm diameter. The remainder occurs over about eight or nine days growth and another doubling of diameter. The spheroid PLMs also show fading of the second PLM peak, which can be due to artefacts, to a progressive loss of labelled proliferating

cells, or to the presence of a slowly-proliferating subpopulation. These possibilities will be discussed further in Chapter 4.

C. Growth Fraction

Growth fraction measurements for spheroids of various sizes and for exponential monolayers are given in Table I. The first column shows values obtained by continuous-labelling with low specific-activity tritiated thymidine for 12 hours. By this method, exponential monolayers have a GF of 0.97. For spheroids, the GF decreased from 0.86 at 100-150 μm diameter to 0.40 at 800 μm. Most of the changes in GF takes place between 150 μm and 400 μm; 400 μm spheroids have a GF of 0.49. Thereafter the decline in GF is more gradual.

An independent determination of GF was made by taking the labelling index of a sample harvested 1 hour after a pulse-label of high-specificity ^{3}H-thymidine. The growth fraction is determined by taking the ratio of L.I. (population)/L.I. (proliferating cells); if T_s (the length of S phase) and T_c are known, L.I. (proliferating) is approximately equal to T_s/T_c. (T_s and T_c for 400 μm and 800 μm spheroids were presented in the previous section.) Values for GF obtained by the pulse-labelling technique are given in the second column of Table I.

The choice of 12 hours as the continuous-labelling time was based on the length of $G_1 + G_2 + M$ and the assumption that the cell cycle parameters in spheroids would be the same as in monolayers. Subsequent estimation of the spheroid cell cycle parameters by means of pulse-labelled mitoses experiments showed that in spheroids, the

G_1 period may be much longer than in monolayers. In fact, for 800 μm spheroids the length of G_1 is 15 hours, significantly longer than the 12 hour labelling time. Thus, the continuous-labelling GF values are underestimates for spheroids greater than 300 μm diameter; this accounts in part for the difference between GF obtained by continuous labelling and by pulse-labelling. This discrepancy, along with a method for correcting for the fraction of cycling cells missed by the 12 hour-labelling protocol, will be given further attention in the Discussion.

D. Cell Shedding

Measured rates of cell shedding for spheroids of three sizes are shown in Table II. The rates of shedding are given in absolute values (number of cells/spheroid-hour) and in terms of percent of spheroid cell number per hour. There is a considerable amount of variability among experiments and even between consecutive samples in the same experiment.

II. SPHEROID RADIATION RESPONSE

A. Suicide Experiments

Figure 4 compares the survival of 'suicide'-treated spheroids and untreated spheroids given various doses of x-rays. The 'suicide'-treated spheroids were treated with high-specific-activity ^{3}H-thymidine to kill cycling cells prior to X-irradiation (see Materials and Methods). Radiation survival of suicide-treated spheroids is corrected for cell-killing due to the suicide treatment.

As can be assessed from the chart, survival of suicide-treated spheroids is not different than that of untreated spheroids, over a range of doses from 200 to 1400 rad. Despite some variations in survival between experiments, within experiments, and within the limits of detection, survivals are the same for the two groups of spheroids.

Preliminary experiments indicated that 16 hours treatment with ^{3}H-thymidine killed approximately 40 percent of spheroid cells (data not shown), about equal to the GF value obtained for 800 μm spheroids (Table I). Subsequently, the PLM studies showed that the length of G_1 in 800 μm spheroids is ~15 hours, raising the possibility that not all cycling cells were killed by the 16-hour suicide treatment. A control experiment was then performed in which cell killing by suicide-treatment alone was studied for treatment times from 12 to 24 hours. Results of the latter experiment indicated that the maximum amount of cell killing by ^{3}H-thymidine was 53-55 percent, and was constant for 18 to 24 hours of ^{3}H-thymidine treatment. A repeat of the suicide-plus-irradiation experiment using a 20-hour suicide treatment yielded the same result (no difference in radiosensitivity between suicide-treated and untreated spheroids) as the previous 16-hour experiments (expt. No. 414 in Fig. 4).

B. Post Irradiation Cell Cycle Progression

Spheroid cultures which had been given a 30-minute pulse-label with ^{3}H-thymidine, were split into two parts. One sample was irradiated, the other not; both samples were returned to the incubator

in separate jars and samples taken as for a pulse-labelled mitoses curve. Similar experiments were done on exponentially growing monolayers. For doses of 500 rad (~50 percent survival) and 800 rad (~20 percent survival), the results are shown in Figs. 5 and 6, respectively. In both spheroids and monolayers, irradiation delayed the entrance of labelled cells into mitosis. In addition, the mitotic index of samples dropped drastically (unpublished observation). At 500 rad, spheroid cells were delayed 4.3 hours, as compared to 2.3 hr for monolayer cells (Fig. 5). Similarly, at 800 rad spheroid cells were delayed 5.1 hr versus only 2.9 hr for monolayer cells (Fig. 6). A repeat of the 500R experiment in spheroids (samples taken only through 12 hr post-irrdiation) yielded the same result as the original trial (data not shown).

DISCUSSION

I. SPHEROID CELL POPULATION KINETICS

A. Measured Kinetic Parameters

Spheroid Growth Rates. The doubling-time of the spheroid lengthens progressively as the spheroid increases beyond 200 μm in diameter (4-5 days old), reaching 140 hours when the diameter is 900 μm (21 days). This is in general agreement with findings in other spheroid systems, most of which have been reported in terms of diameter or volume measurements (19-21,70). The method used here was to enumerate cells per spheroid versus time, which is a more sensitive method than diameter or volume for purposes of kinetic analysis. For example, the slope of diameter increase vs. time is shallower for spheroids <300 μm than for those above 300 μm (20; Fig. 2a), even though the cell population doubling rate is faster for the smaller spheroids. In the early stages of spheroid growth, the volume of individual cells is decreasing; at diameters above 400-600 μm (depending upon cell line) a significant volume of acellular necrotic matter may be present. Thus, volume is not necessarily proportional to cell number. Of course, for studies of tumors *in vivo*, volume measurement is the only practical method.

The spheroid cell population growth curve for 9L cells has three distinct regions: an early region of exponential growth, a middle region where the T_D increases continuously, and a late region demarcated by a sharp increase in T_D between days 14 and 16 of growth. This 3-stage growth pattern was observed for both culture

types: controlled low-density cultures in which the number of cells per ml of medium was kept at approximately 1.5×10^5, and high-density cultures in which the cell number exceeded 10^6/ml by day 11 of culture. (The density referred to herein is culture density in terms of number of cells per ml of medium.) However, the growth curve for spheroids grown under conditions of high cell density shows a distinctly earlier onset of the late region of growth, but the values of T_D in the late region are the same (within experimental limits) as those for the late region of low-density culture spheroids. Spheroid growth in the early and middle regions is not significantly altered by growth under high density (it should be noted that the two culture types are initiated at equal densities; in the cultures where cell density is not controlled, cell density exceeds the control density by a factor of 4 by about days 11-12).

The data most directly comparable to those presented here are those of Durand for V79 cells (63). In that report, a plot of cell number per spheroid versus time shows three regions analogous to those just described for 9L cells. For V79 cells, however, T_D increases more drastically in that late region, reaching 490 hours by day 25 (approx. 700 μm).

The three regions of the 9L spheroid growth curve can be correlated with changes in several kinetic parameters (GF, T_C, ϕ) for which values were obtained over the entire range of growth. A discussion of such correlations will appear following the sections on individual kinetic parameters.

The rate of diameter increase for 9L spheroids is linear at approximately 55 μm/day over the range from 300 to 1000 μm (Fig. 2a). This is quite close to the rate of 50 μm/day reported for EMT6 spheroids (70), double that reported for V79 spheroids (63), and in the middle of the range of diameter growth rates reported for seven lines of mouse mammary tumors (19). 9L spheroids grown by Deen et al. had a much slower rate of increase in diameter (21). The difference between their results and mine are almost certainly due to differences in the methods of culture, especially in terms of feeding schedules. There are also discrepancies between the values of kinetic parameters obtained for 9L cells here and those reported by Deen et al.; the possible reasons for these discrepancies will be fully discussed in a later section.

The linearity of the diameter vs. time curve for 9L spheroids is also found for other spheroid types (see above; 19-21,70) as well as for many tumors *in vivo* (5). Such linearity can be accounted for by the model of Conger and Ziskin (20), which is based on the assumption of a constant thickness of the dividing layer. However, other models for spheroid and tumor growth also predict linear increase in diameter (5,70,71).

Cell Cycle Parameters. My results indicate that cells in 9L spheroids undergo a considerable lengthening of the cell cycle time as compared to the cell cycle time of monolayer cells. In the data presented here, the lengthening is from 16.6 hr (monolayer T_c) to 24 hr (400 μm spheroids) to 28 hr (800 μm spheroids); nearly a factor of 2.

These data contrast with those of Deen et al., who reporteed that for 9L spheroids up to 600 μm diameter, there was no significant change in cell cycle parameters from those of monolayers (21). In my PLM curves, the lengthening takes place entirely in the G_1 phase; S and G_2 are the same as for cells in monolayer. Artefacts which could result in an apparent lengthening of the 'trough' of the PLM include underexposure of autoradiographs from later time points and/or a too-high threshold for counting cells as labelled. However, doubling the exposure time or decreasing the threshold produced noisy and inconsistent counts in the trough region with no convincing evidence that the 2nd peak is located earlier than as shown in Fig. 3c (data not shown).

Cells in V79 spheroids also undergo a lengthening of T_c, but the degree of change is less, from ~16 hr in monolayers to 20 hr in 700 μm spheroids (63). In solid tumors it is generally found that T_c remains the same over a wide range of tumor growth, and is the same as for _in vitro_ monolayers. However, there are exceptions to the rule of similar T_c for tumors and _in vitro_ cultures of the same cell line. Cells in the center of a rat rhabdomyosarcoma had a T_c of about 26 hours as compared to T_c of 18 hours for cells near the periphery (69). Similar studies of KHJJ and EMT6 tumors also reported that cells in nutritionally-deprived regions had an elongated T_c, but the degree of elongation was not so large (136). Mouse ascites tumors, which have been adapted by repeated passage in the peritoneal cavity to growth under rather unusual conditions, consistently show a

lengthening of T_c with time after implant (5). However, in ascites tumors the elongation appears in S and G_2, as well as in G_1; in the other cases described above lengthening is confined to the G_1 phase. As yet no measurements of T_c in 9L tumors have been published.

The lengthening of T_c in solid tumors is associated with the location of cells in nutritionally deprived regions; inadequate nutrition has also been implicated as a factor in the elongation of T_c in ascites tumors (5). The elongation in T_c reported here is unlikely to be due to inadequate nutrition, particularly for 400 μm spheroids in which T_c is already considerably increased. Nor is growth under low pO_2 likely to be the cause, since 9L spheroids contain <3 percent hypoxic cells (21,119,130). Other factors may be involved: for example, growth in altered pH environments has been reported to increase the doubling-time of monolayers (61,62,79).

Further inferences concerning the cycling cell population in 9L spheroids can be drawn from a closer examination of the PLM curves for 400 and 800 μm spheroids. The first peak is quite high and the trough quite low: this suggests that there is little variability in G_2 or S and that label did sufficiently reach all cycling cells. However, the second peak is only about 60 percent as high as the first peak; this phenomenon has been termed 'fading'. Fading can be the result of the artefacts already mentioned: inadequate exposure of late-time autoradiographs or too-high threshold for counting. As previously mentioned, neither of those is believed to be the case here. Fading

can also occur if heavily-labelled cells accumulate sufficient radiation damage to prevent their further entry into mitosis (5). However, since 16 hours of labelling at 1 μCi/ml, 20 Ci/mmole ^{3}H-thymidine reduced cell survival by only 50 percent (suicide experiments), it seems unlikely that 30 minutes of labelling at 1 μCi/ml, 6.7 Ci/mmole would cause the degree of fading seen here. Aside from these artefacts, there are two possible biological explanations for fade. First, there may be a significant variability in T_c; it has been found that T_c in 9L monolayers, while having an average value of 19.5 hr, varies from 11 to 35 hours (124). This variability would be expected to lower and spread the second peak. Second, if cells which were nonproliferating during the pulse-label now re-enter the proliferating compartment, fade of the 2nd peak would result. One or both of the above phenomena may occur in 9L spheroids.

The method of pulse-labelled mitoses is generally considered as providing the best characterization of cell cycle phase and T_c; however, the PLM technique primarily measures the parameters of the most rapidly proliferating cells. It is insensitive to slowly-cycling subpopulations, and other methods of kinetic analysis may give different results for mean T_c than PLM curves. Recently, it has been reported that PLM data from a mouse carcinoma underestimated the mean T_c by a factor of 2 compared to other techniques (137). The finding was supported by independent evidence comparing values of cell loss factor derived from PLM data vs. direct measurement by ^{125}I-labelling (138). This insensitivity of the PLM method to slowly-

proliferating subpopulations should be kept in mind in any discussion of tumor kinetic parameters derived from PLM data.

Growth Fraction. Most of the measurements of growth fraction were made using a continuous-labelling method, which may lead to overestimation of GF at very long labelling times (5). This artefact arises when some of the daughters of labelled proliferating cells enter the nonproliferating compartment prior to sampling. Since they contain label incorporated by the parent, they are counted as proliferating even though they are themselves nonproliferating. Under conditions where the oldest nonproliferating (unlabelled) cells are being steadily lost, the continuous-labelling curve will eventually tend to 100 percent labelling (5). If cell loss is very slow, the curve will appear to plateau at a level below 100 percent; some authors (for example, Deen et al. [21]), have taken the plateau level as the growth fraction, but we believe this to be an inappropriate method. A valid estimate of growth fraction can be obtained from the continuous labelling curve by extrapolating the slowly-rising component, back to the y-axis (5) or by fitting the data to an appropriate model (63).

Instead, I attempted to develop a less cumbersome continuous-labelling technique for GF measurement: to label for a period equal to $G_2 + M + G_1 + 4$ hr. Such a labelling time should allow all actively-cycling cells time to enter S and incorporate sufficient label for autoradiographic detection, yet minimize the contribution of labelled-nonproliferating daughters to the labelling index. Since there was reason to believe, from the data of others, that the spheroid

cell cycle parameters would be the same as for monolayer, the labelling time used for all GF experiments was 12 hours. In 9L monolayers, this labelling-time gave a GF value of 0.97, the same as that previously reported for 9L monolayers (21).

Subsequent PLM experiments on spheroids, however, indicated that the G_1 period in spheroids may be much longer than in monolayer. So, the GF measurements for spheroid sizes over 250 μm are probably underestimates of the true values. Still, the values in Table 1 show a steady decline from 0.86 for 150 μm spheroids to 0.40 at 800 μm, with over two-thirds of the drop in GF occuring by 400 μm diameter.

An alternate measurement of GF is available for spheroids where T_c, T_s (the duration of S-phase) and pulse-labelling index are known. The growth fraction is equal to the ratio of L.I. of the entire cell population to L.I. of the proliferating cells (5). L.I. proliferating can be estimated as T_s/T_c; then L.I. population/T_s/T_c equals GF. The data on T_s, T_c and L.I. population are available from the PLM experiments on 400 μm and 800 μm spheroids; the GF values obtained from these data are indeed somewhat higher than those from the 12-hour continuous-labelling.

It is possible to estimate the fraction of cycling cells 'missed' by the 12-hour labelling time, given a knowledge of the actual cell cycle parameters. For example, in 400 μm spheroids where G_1 = 11.6 hr, the cycling cells which are in G_2 + M at the time of addition of label will not yet have become labelled after 12 hours. The fraction of G_2 + M cells in the total cycling population can be

estimated as T_{G_2+M}/T_C: for 400 μm spheroids 3h/24h = 12.5 percent missed cells. Now, the 12 hr-L.I. = 0.49 = 87.5 percent of the 'true' value and by a simple proportionality the 'true' value of GF would be 0.56. This is still somewhat below the estimate of 0.67 from the PLM-L.I. data, but within the various errors of estimation. For 800 μm spheroids, not only G_2 + M cells but cells in the first 3 hours of G_1 are 'missed' by the 12 hr labelling time. Calculations as described above yield a corrected GF of 0.51 (as compared to the value from PLM-L.I. data of 0.49). Table 3 displays values of GF obtained from 12 hr-labelling, from 12 hr labelling corrected for 'missed' cells, and from PLM-L.I. data. For 225 μm, 300 μm, and 500-600 μm spheroids, where no direct measurement of T_C is available (the latter is necessary for correcting the 12 hr GF as well as calculation of GF from PLM-LI) upper limit values for corrected GF are given.

Regardless of which GF method is used, it is clear that there is a progressive decrease in growth fraction of 9L spheroids as they grow from 100 to 900 μm in diameter. Most of the change in GF occurs between 150 μm and 500 μm; a decline from 0.86 to approximately 0.50. These changes are similar to those reported for V79 spheroids in which GF gradually declined from 0.93 at day 1 to 0.39 at day 25 (~800 μm diameter). However, Deen et al., reported that for 9L spheroids the growth fraction was constant at approximately 0.5 over the range from 200 to 500 μm (21).

In summary, then, the growth fraction studies indicate that GF decreases over the range of growth from 150 to 500 μm and then remains roughly constant from 500 μm to 800 μm at about 0.5. This value is similar to the GF observed for 9L intracranial tumors in vivo. The decreases in 9L growth fraction are not due to hypoxia, since radiobiological studies indicate that there are <3 percent hypoxic cells in 9L spheroids (21,119,130). Thus, other factors, possibly including build up of toxic byproducts, inadequate penetration of glucose or other essential nutrients, and pH effects, must be involved in causing cells to enter a dormant state. The 9L data reported here differ from the data of Deen et al. on 9L spheroids; this is probably due to differences between the methods of initiation and maintenance of 9L spheroids used by Deen et al. and those employed here. The pattern of decreasing GF and the range of GF values found here for 9L cells is similar to those reported for V79 spheroids (63). These findings (both the 9L data presented here and the V79 data of Durand) are in agreement with the constant-crust model for spheroid growth (20). This model, based on the assumption of a constant thickness of the dividing layer, predicts a decreasing growth fraction.

Discrepancies Between the Data of Deen et al. and Myself

The discrepancies between the data of Deen et al. (21) and those presented here for growth rate, T_c and GF in 9L spheroids is probably due to differences in culture methods and/or serum content of the medium. For example, 9L monolayers grown in 20 percent fetal calf serum had a T_c of 12-1/2 hr (139); 9L monolayers grown in 10 percent

fetal calf serum by Deen et al. had a T_c of 19.5–20 hr. 9L monolayers used in these experiments were grown in 15 percent total serum (12.5 percent newborn calf, 2.5 percent fetal calf) and a T_c (from PLM data) of 16.6 hours, which agreed well with the monolayer doubling-time of 16 hours (data not shown). With the 9L tumor line, which is known to be rather unstable, the possibility of differences between 9L-SF cells and mine must be considered (124). The cells used here were initially obtained from Deen at an early passage after thawing from their frozen stock. Samples were then prepared and frozen, still at passage 5–6 or less; subsequently my 9L cells were renewed every 3 months from these secondary frozen stocks. Stock cultures were maintained as described by Wheeler et al. (124) to avoid changes in the cell population. The possibility that such changes did occur cannot, however, be ruled out.

The differences in growth rate are more likely to be due to the differences in spheroid culture methods between Deen et al. and myself than to differences in the serum content or lot; spheroid growth rates were insensitive to serum content from 5 to 20 percent under the culture conditions of Deen et al. (21). In this laboratory, growth rates of 9L monolayers differed by only an hour or two for cells grown in 10 percent FCS, 12.5 percent NCS–2.5 percent FCS, or different serum lots (Sweigert, unpublished data). The differences between spheroid culture methods employed by Deen etal. and by myself are, however, quite pronounced. Deen et al. started their spheroids as single-cell suspensions in spinner flasks; after 3 weeks populations

of mean diameter 200 μm and 300 μm were selected (from an initial population that included spheroids over 500 μm diameter) for use in experiments. In our laboratory, spheroid cultures are initiated by the method of Yuhas and Li (140), in which cells are seeded into agar-coated dishes and incubated for two days, until small aggregates (generally $\leq$50 μm diameter) are formed. These aggregates are then transferred to suspension culture, and by 3 weeks after initiation are over 800 μm in diameter. Thus, the spheroids used in the experiments of Deen et al., are much older in terms of days in culture than spheroids of equivalent size studied here. Furthermore, the feeding schedule followed by Deen et al. was once every 3-4 days beginning one week after seeding 3×10^6 cells/250 ml medium in spinner jars. 9L spheroids in this study were initiated at slightly higher cell densities, but were fed daily beginning two days after transfer to spinner jar. If the feeding schedule, even in the first week of spinner culture, were reduced to every 3-4 days, the spheroid growth rate showed a significant drop (data not shown). Similarly, if spheroid cell cultures were allowed to reach high cell densities, a condition partially analogous to a reduced feeding schedule), the spheroids entered the 'late' region of growth at a smaller size. One might speculate then that the culture methods used by Deen et al. produced 9L spheroids which were more 'mature' in terms of kinetic properties at small sizes as compared to spheroids characterized in my work. This would account for the differences in GF and spheroid growth rate between 9L spheroids of Deen et al. and myself. However,

the lengthening of T_c in 9L spheroids observed here but not by Deen et al. is not satisfactorily accounted for by either the differences in culture methods or serum content.

B. ESTIMATION OF CELL LOSS FACTOR

The rate-constant for cell loss (K_L) and the cell loss factor ϕ (defined as K_L/K_p, where K_p = rate constant for cell production) for spheroids of different sizes were calculated from measurements of the kinetic parameters already discussed--T_D, T_c and GF; the formula used for the calculation and its derivation are given in Appendix A. Values of K_L and of ϕ are for spheroids of different sizes are shown in Table III. Since the continuous labelling GF measurements were underestimates of the true GF, the PLM-L.I. values and/or GF estimates corrected for the fraction of 'missed' cells were used in the calculations of cell loss. Furthermore, since T_c was not constant and was measured only for 400 μm and 800 μm spheroids, upper and lower values for ϕ based on the upper and lower limits for T_c are given for spheroids of other sizes. For spheroids <200 μm, there is essentially no cell loss. For spheroids from 220 μm to 500 μm, there is some cell loss, with upper limits of about 0.15 for ϕ; the true value is probably somewhat less. The rate of cell loss in this range is similar to the measured rate of cell shedding; thus, most of the cell loss is probably due to shedding and not to cell death. Above 600 μm the rate of cell loss increases sharply, with ϕ = 0.5 for 800 μm spheroids. At this point, then, the number of cells lost per unit time is equal to one-half the number of new cells produced. The rate of cell loss is also considerably higher than the

rate of cell shedding (a factor of 3 or more), so that it seems likely that most of the increase in cell loss is due to cell death. The values of the cell loss factor found here for 9L spheroids are rather less than those reported for V79 spheroids, where ϕ is about 0.5 by day 6 (300 μm). By Day 25 (700 μm), ϕ is nearly 0.9, so that cell production is nearly balanced by cell loss (63).

For tumors in vivo, reported values of ϕ range from 0.1 to 0.9. Many of these estimates of ϕ are calculated from PLM and T_D values. The precision of estimates of ϕ is notoriously low, but in general ϕ increases with tumor size and tumor-doubling time (5), as is reported here for spheroids. Recently, it has been reported that PLM data, which primarily reflect the kinetic properties of the fastest-cycling cells, may underestimate the mean value of T_c by as much as a factor of 2 compared to T_c values from other techniques (137). One implication of this finding is that values of ϕ obtained using PLM data may be too high by a factor of 2. In mouse carcinoma NT tumors, there is evidence that values of ϕ obtained by PLM data were about twice as great as values obtained by measurement of the rate of loss of ^{125}IUdR (138). It should be kept in mind that measurement of cell loss by the ^{125}IUdR technique may be subject to several potential artefacts, including re-utilization (of label released by dead cells within the tumor or from rapidly turning-over host tissues such as the gut) and influx of labelled host cells. Any of these artefacts could lead to artificially low values of cell loss rate. Influx of labelled host cells has been shown to be a significant

influence on ^{125}I measurements in EMT6 and KHJJ tumors, but not for RIF-1 (141). It is generally thought that re-utilization of ^{124}I label occurs at very low efficiency, with little effect on rates of ^{125}I loss (68), but it has not been entirely ruled out.

Nonetheless, the discrepancy between T_c's obtained by PLM or by other techniques and the evidence (for the same tumor line) that ϕ-values derived from PLM data differ from ϕ-values obtained by direct measurement in the way predicted by the difference in T_c may be very significant. Since the PLM tchnique is insensitive to slowly-cycling subpopulations, estimates of ϕ obtained from PLM data may be greatly overestimated for many tumor or spheroid systems. The PLM data persented here certainly indicate that under some conditions the T_c of 9L tumor cells can be greatly lengthened. In terms of the values for ϕ derived from these PLM data, two potential sources of error exist. First, some of the GF values are based on PLM data; these are similar however to estimates based on continuous-labelling data which should be more sensitive to slowly-cycling cells. Therefore, the GF values are not likely to be causing error in the estimates of ϕ. A second source of potential error is the possibility that in 9L spheroids there is a significant fraction of slowly-cycling cells whose T_c is even longer than that derived from the PLM data. Then, the rates of cell production and accordingly of cell loss may be overestimated. As discussed earlier, the PLM curves obtained here can be interpreted as evidence for substantial variation in T_c among 9L spheroid cells or that there is movement from the nonproliferating

state back to a proliferating state. If this is the case, then it would be more accurate to consider the values of ϕ and GF as reflecting the average properties of the 9L spheroid cell population.

The rate of cell shedding in 9L spheroids (Table 2) is far less than that of EMT6 spheroids, where shedding reduces the rate of increase in diameter by up to 50 μm per day (73).

C. Summary: Dynamics of 9L Spheroid Growth

The data on kinetic parameters collected over an extended period of culture allow one to draw a detailed picture of the dynamics of spheroid growth. In the early stage (<200 μm), growth is exponential and similar to that of exponential monolayers, with a high growth fraction and virtually no cell loss. Since the T_D is 19 hours, it is sensible to assume that the average cell cycle time does not exceed 19 hours and is probably very similar to the monolayer T_c of 16.6 hours. Just beyond 200 μm, the doubling-time increases sharply to 28 hours. This increase in T_D is due to a drop of 17 percent in growth fraction and a slight increase in cell loss, both of which occur in the 200-250 μm growth range. Probably T_c is beginning to increase, too, though I have no data specific to this point. The oxygen diffusion distance in tissue is approximately 100 μm, and proliferative zones in tumors *in vivo* generally extend about 100 μm from capillaries (2,3). Thus, the changes in GF and ϕ which occur as the spheroid increases beyond 100 μm radius are probably related to the same conditions of inadequate nutrition and oxygenation which occur in tumors.

Between 200 μm and 600 μm, the doubling-time increases progressively to 54 hours, due primarily to further decreases in the growth fraction and lengthening of the cell cycle. The cell loss factor remains relatively low and constant during this period; most of the cell loss can be accounted for by shedding from the spheroid surface. Beyond 600 μm, T_D again increases sharply, to 91 hours at 700 μm and 110 hours at 800 μm. In this region, the increased T_D is not due to further decrease in GF or to the slight further increase in T_C. Therefore, the increased T_D must be largely due to an increase in cell loss factor, which is shown by calculation to be 0.5 at 800 μm, much higher than for spheroids $\leq$600 μm. Cell shedding here accounts for only 15 to 30 percent of the total cell loss; the remainder is presumably due to cell death within the spheroid.

One implication of these findings is that cell death is not occurring to a large extent in spheroids below 600 μm in diameter. The plot of cell number per spheroid versus volume is linear from about 300 to 700 μm; above 700 μm it becomes more shallow, which would be consistent with an increase in the amount of acellular necrotic material in the core. Spheroids cultured at very high densities enter the 'late' region of growth (as defined by a rapid increase in T_D to 110 hr) sooner than spheroids cultured at low density. No kinetic measurements aside from T_D were done on these high-density cultures but by analogy to the late region in the well-characterized low-density-culture spheroids, cell death is probably the reason for the earlier shift into the mature phase of growth of the high-density

spheroids. It seems logical that under conditions of greater nutritional deprivation such as those arising in very high density cultures, the inner cells in spheroids may begin to die at smaller spheroid sizes.

The usefulness of the 9L spheroid system is proportional to the degree that 9L spheroids mimic the properties of 9L tumors *in vivo*. The results reported here, particularly the lengthening of T_c, should be verified *in vivo*. No report of PLM data in 9L tumors has yet been published. However, the growth fraction in 9L tumors weighing 60–80 mg has been reported to be 0.47, similar to the value reported here for spheroids $\geq$500 μm (21,124). The observation that significant cell death in 9L spheroids occurs only at diameters above 600 μm is consistent with the observation that very little necrosis is present even *in vivo* in 9L tumors weighing up to 2 grams (114). With the exception of the increases in T_c seen in these 9L spheroids, the progressive changes in GF and ∅ seen here are qualitatively similar to kinetic patterns in many tumors.

The data acquired in this study have not been fitted to any models of spheroid or tumor growth. However, the data appear consistent with several models. The constant-crust model of Conger and Ziskin (20) predicts a linear rate of increase in diameter and a progressively decreasing growth fraction; both features are found in the 9L data reported here. The model of Curtis based on kinetic parameters is likely to fit these 9L data, and could also produce a framework for

studying post-irradiation proliferation in spheroids (69). A model based on parameters of crust thickness and cell shedding may also fit 9L spheroid growth (70).

II. SPHEROID RADIATION STUDIES

A. Radiation Sensitivity of Quiescent Cells

The radiosensitivity of quiescent cells in 9L spheroids appears to be the same as that of the cell population of 9L spheroids as a whole, within the limits of the experimental data. The presence of a quiescent subpopulation cannot account for the radioresistance of 9L spheroids compared to monolayers. It was possible to ascertain this in 9L spheroids because they contain a negligible fraction of hypoxic cells and because the radiation response curves are not complicated by a pronounced cell age-response.

In these experiments, quiescent cells are defined by their failure to be killed by 16-20 hours of exposure to 1 μCi, 20Ci/mmole ^{3}H-thymidine. The experiment was performed in 800 μm spheroids, which have approximately equal proportions of cycling and noncycling cells (Table 3, GF ≃ 0.50). Assuming all of the cycling cells are killed by the suicide treatment, a difference in radiosensitivity between cycling and noncycling cells of a factor of 2 or more should be detectable in these experiments (calculation not shown).

Although there is variability in survival to a given dose between experiments, particularly at low doses, within experiments the survivals of the two samples are not significantly different. Furthermore, fitting of survival curve parameters to the compiled data

for the two samples indicates that both conform to the parameters of the radiation survival curve, D_0, n, and D_q previously reported for 9L spheroids in this laboratory (119,130).

The 16-hour interval for ^{3}H-thymidine treatment was chosen because preliminary experiments showed that 16 hours of treatment was sufficient to yield a survival level in treated spheroids equal to 1-GF. However, as previously discussed, the GF values obtained after 12 hr-continuous labelling were underestimates. Thus, up to 15 percent of the cycling cells may have survived the treatment, further reducing the potential resolution of the experiment. A subsequent experiment indicated that 20 hours of thymidine treatment resulted in a surviving fraction of .53 which was not further reduced by additional treatment up to 24 hours. One radiation and suicide experiment (No. 414) was done using a 20-hour treatment; the resulting data still indicated no difference between the radiation survival of quiescent cells and that of the spheroid as a whole.

A further potential complication was the possibility that the quiescent cells, presumably concentrated in the inner region of the spheroid, might have a lower plating efficiency than the cycling cells which were concentrated in the outer well-nourished zone. A control experiment in which a two-step dissociation of spheroids designed to separate the outer 50 percent of cells from the inner 50 percent was done, and the two fractions tested separately for colony-forming efficiency. CFE's of the outer and inner cells were nearly identical (0.49 ± 0.58 vs. 0.46 ± .029). Although it has been reported that

inner cells in EMT6 spheroids have a reduced CFE (18), inner cells in V79 spheroids have the same CFE as outer cells (50,120).

The finding that cycling and noncycling cells in 9L spheroids have the same radiosensitivity is consistent with the fact that 9L spheroids from 150 to 600 μm yield the same radiation-survival curve (130), despite the wide variaton of GF over this size range. In V79 spheroids, radiation cell survival vs. depth in the spheroid has been carefully studied (121). The innermost 10 percent are most resistant but this is probably due to hypoxia (ibid).

B. Radiation-Induced Division Delay

The results of PLM experiments on X-irradiated monolayer and spheroid cells clearly show that 9L cells grown as spheroids experience a radiation-induced division delay (RIDD) twice as long as that of cells grown as monolayers (Figs. 5 and 6). This longer delay is not the result of greater damage sustained by spheroid cells, since under the same irradiation conditions survival was a factor of 2 lower for monolayers than for spheroids (data not shown). This finding contrasts with reports that radiation-induced delay in V79 spheroid cells is less than delay in V79 monolayer (128,130). For V79 spheroids and monolayers treated with 60-Co γ-rays, data from postirradiation cell-counting experiments were fitted to a mathematical model; the results showed that delay was less in spheroid cells than in monolayers by nearly a factor of 3). The methods most often used to quantitate radiation-induced division delay are time-lapse cinematography, and yield of mitotic cells by sequential mitotic shake-off. These two

methods are obviously unsuitable for spheroids; the method chosen for this study of RIDD in 9L spheroids and monolayers was that of pulse-labelled mitoses, which provides information about the progression of cells irradiated in S-phase into mitoses.

The method used for the initial V79 studies of RIDD were cell count measurements made at 96 hours post-irradiation. One might expect such measurements to be rather insensitive to delays of 10-15 hours or less which could be expected over most of the dose-range (T_c of V79 cells $\leq$18 hr). Dose-response curves for 96 hr post-irradiation cell-counts closely paralleled that for cell killing in 300 μm spheroids, which would be consistent with the idea that 96-hr post-irradiation cell counts mainly reflect cell-killing and not radiation-induced delay.

Studies of V79 spheroids and monolayer cells irradiated with heavy ions and analyzed by flow cytofluorimetry (FMF) also indicated that outer spheroid cells were blocked less than monolayer cells for the same dose (127). In the latter study, a fractionated trypsinization was used on spheroids so that the kinetic response outer (presumed mostly cycling) cells and inner (noncycling cells) could be analyzed separately. The authors hoped by this means to avoid an artefact whereby the presence of a large noncycling population of cells with G_1-DNA content might mask the post-irradiation buildup of cycling cells in the G_2+M compartment. In fact, FMF analysis of the inner cell fraction did indicate that no significant kinetic changes took place until 100 hours or more following irradiation (127). With

regard to the decreased blockage of outer spheroid cells as compared to monolayers, it could not be ruled out that contamination of the outer cell fraction by noncycling cells was the cause of the quantitatively smaller kinetic response of the spheroid cells as compared to monolayer cells (128). In any case, FMF histograms do not yield information about the progression of individual cells within the population. For example, FMF histograms of 800 μm 9L spheroids at various times following irradiation showed almost no changes (Rodriguez, unpublished data). Thus, the reports of reduced G_2-delay in V79 spheroids are not entirely conclusive.

It is generally thought that radiation blocks cells in G_2, but the data presented here do not distinguish between a block in late S-phase and a block in G_2. The data points for only two doses each in spheroids and monolayers do not provide sufficient basis for a comparative dose-response analysis. However, the durations of RIDD for 9L spheroid and monolayer cells are both somewhat less than those reported for various cell lines using techniques other than PLM (97,98,100,101). Since the length of RIDD is dependent upon the cell age at irradiation, and less for cells irradiated in S-phase than in G_2 (101), it is difficult to compare quantitatively the results obtained here by PLM method and those obtained using other techniques, most of which reflect mainly the delay of cells irradiated in G_2.

The mechanism for the enhanced RIDD in 9L spheroids compared to monolayers is unknown. Most evidence suggests that the target for RIDD is in the DNA or some structure very closely related to DNA

(97,101-104,106). One possibility is that the difference in RIDD is related to differences in cAMP between spheroids and monolayers. Cyclic AMP is known to play a role in several aspects of cell cycle progression (32,37); it has been shown that activity of adenyl cyclase (an enzyme which plays a role in the control of cellular cAMP levels) is significantly lower in spheroids than in monolayers (14). Although a direct role for cAMP in modification of RIDD has been ruled out (152,156), one recent report presents evidence that the ratio of cAMP to cGMP may be significant (152). Two other hypotheses have been suggested, based on the relationship between the magnitude of RIDD and the degree of x-ray cell killing observed in AT cells, caffeine-treated normal cells and untreated normal cells (145,148). These hypotheses will be discussed under the heading G_2 Delay and Cell Survival.

In a purely empirical way the longer RIDD observed in cells grown as spheroids has implications for the clinical radiotherapist. If the radiation age-response and partial synchrony induced by a previous radiation-dose are to be exploited, knowledge of the RIDD kinetics is important. The comparison of RIDD in 9L spheroids and monolayers reported herein suggest that RIDD may be significantly longer in tumors *in vivo* than in monolayers *in vitro*. Of course, this result should be confirmed in spheroids and tumors of other cell lines. As to previous studies of RIDD in tumors, I could find only one such study, done on Erlich Ascites tumors (99). This study did not compare *in vivo* and *in vitro* monolayer delays, but the length of x-ray induced G_2 delay was much longer than that reported for PLM studies of other

cell lines *in vitro* about 1 hour/100 rads (similar to values obtained for 9L spheroids in this report). The significance of the extended RIDD in 9L spheroids depends in large part on whether the phenomenon is observed in 9L tumors compared to monolayers; such studies should be undertaken.

C. G_2-Delay and Cell Survival

The G_2-delay has been hypothesized by several authors to be a period of cell recovery (145,146,149,155). If the G_2-delay induced by radiation does have an influence on cell survival, the finding made here that 9L cells grown as spheroids have a greater RIDD than cells grown as monolayers may provide an explanation for the greater radioresistance of spheroid cells as compared to monolayers. The longer G_2-delay in spheroid cells may allow them more time to repair potentially-lethal damage before it is fixed by passage through mitosis.

Many studies show that at nontoxic levels caffeine reduces or eliminates radiation-induced G_2 delay while synergistically enhancing cell killing (145,149,152,155). Caffeine enhancement of cell killing appears to occur only in G_1 and G_2, and to a much greater degree in G_2 (149). Caffeine must be present continuously to have this effect; it allows the damage leading to G_2-delay to be bypassed but apparently also prevents repair of the damage. The latter is inferred from the observation that when caffeine is removed a G_2-delay of the duration normally expected is manifested (145).

Further evidence for the role of G_2-delay in cell survival comes from studies of ataxia telangiectasia (AT) cells. AT is a heritable syndrome which has an abnormally high radiosensitivity as one of its primary characteristics. AT cells exhibit little or no G_2-delay in response to radiation, but high radiosensitivity, compared to normal cells (146,147). The lack of radiation-induced G_2-delay in AT cells has been suggested as a reason for their abnormal radiosensitivity (148). The mechanism(s) involved in the reduction of G_2-delay and simultaneous enhancement of cell killing in AT cells and caffeine-treated normal cells is unknown, but two possibilities have been suggested. First, that G_2-delay and inhibition of DNA synthesis are the result of damage to (or changes in) chromatin configuration due to irradiation; AT cells are postulated to have some defect in chromatin coiling and caffeine to act upon lesions affecting chromatin configuration in irradiated normal cells so as to mimic the defect in AT cells (145,148). Second, that poly(ADPR) synthesis is involved; caffeine is a strong inhibitor of poly (ADPR) synthetase, and AT cells may be deficient in synthesis of poly (ADPR) following irradiation (145). Studies of G_2-delay in 9L spheroids and monolayer cells may help in elucidating the mechanisms governing RIDD.

Results of recent studies comparing PLD repair in 9L spheroids and monolayers are consistent with the idea that the longer G_2 delay in spheroid cells may be a factor in their enhanced survival. It has been found that if 9L monolayers are allowed to repair x-ray induced PLD, their survival approaches that of 9L spheroid cells. In contrast,

9L spheroid cell survival was not enhanced by a post-irradiation repair period (157). It seems unlikely that the lack of increase in x-ray cell survival in spheroids after post-irradiation holding is due to an inability to repair PLD, since 9L spheroids (but not monolayers) did exhibit PLD repair following high-LET irradiation (156). One interpretation of the x-ray results is that under standard irradiation plus immediate assay conditions, 9L spheroid cells can repair x-ray induced PLD without any post-irradiation holding, and such PLD repair can largely account for the difference in radiosensitivity observed between spheroid cells and monolayers in immediate-plating experiments. The speculation advanced here is that the longer G_2 delay in spheroids may be a factor allowing spheroids to repair PLD without a post-irradiation holding period.

APPENDIX A: Cell Loss Factor

As defined by Steel,

$$\phi = \frac{K_L}{K_p} \text{ where } K_L = \text{rate constant of cell loss}$$

K_p = rate constant for cell production

Simple exponential growth:

$$\frac{dN}{dt} = \lambda N \quad , \quad \lambda = \frac{\ln 2}{T_c} \qquad T_c = \text{cell cycle time for individual cells}$$

Equation modified for growth fraction <1 and cell loss:

1) $\frac{dN}{dt} = \underset{k_p}{\lambda\ GF\ N} - \underset{K_L}{\gamma N}$ where GF = growth fraction

2) $N(t) = N_o e^{(\lambda\ GF - \gamma)t} \longrightarrow$ 3) slope $= \lambda\ GF - \gamma = \frac{.693}{T_D}$ where

T_D= doubling time of spheroid cell population

Rearranging 3)

4) $\gamma = \lambda\ GF - \frac{.693}{T_D}$ where λ, GF, and T_D are all measurable quantities

5) $\phi = \frac{\gamma}{\lambda\ GF}$ $\qquad (\gamma = K_L \quad , \quad \lambda = GF = K_p)$

BLBLIOGRAPHY

1. R. M. Sutherland, J. McCredie, and W. R. Inch. Growth of multicell spheroids in tissue culture as a model of nodular carcinomas. J. Natl. Cancer Inst 46, 113-120 (1971).

2. R. H. Thomlinson and L. H. Gray. The histological strucute of some human lung cancers and the possible implications for radiotherapy. Brit. J. Cancer 9: 539-549 (1955).

3. I. F. Tannock. The relation between cell proliferation and the vascular system in transplanted mouse mammary tumor. Brit. J. Cancer 22: 258-273 (1968).

4. R. M. Sutherland and R. E. Durand. Radiation rsponse of multicell spheroids, and in vitro tumor model. Curr. Topics Rad. Res. Quarterly 11, 87-139 (1976).

5. G. G. Steel. Growth Kinetics of Tumors, Oxford University Press (1977).

6. S. Rockwell and R. F. Kallman. Cellular radiosensitivity and tumor radiation response in the EMT6 tumour cell system. Radiat. Res. 53: 281-294 (1973).

7. R. P. Hill, R. Ng, B. F. Warren and R. S. Bush. The effect of intercellular contact on the radiation sensitivity of KHT sarcoma cells. Radiat. Res. 77: 182-192 (1979).

8. R. E. Durand. Cure, regression and cell survival: a comparison of common radiobiological endpoints using an in vitro tumour model. Brit. J. Radiol. 48: 556-571 (1975).

9. J. Denekamp. Experimental Tumor Systems: Standardization of Endpoints. Int. J. Rad. Oncol. Biol. Phys. 5: 1175-1184 (1979).

10. L. H. Gray, A. D. Conger, M. Ebert. Concentration of oxygen dissolved in tissues at time of irradiation as a factor in radiotherapy. Brit. J. Radiol. 26: 638-648 (1953).

11. E. J. Hall. Radiobiology for the Radiologist, 2nd edition, Harper and Row, Hagerstown, M.D. (1978).

12. E. M. Rottinger and M. Mendonca. Radioresistance secondary to low pH in human glial cells and Chinese hamster ovary cells. Int. J. Rad. Oncol. Biol. Phys. 8: 1309-1314 (1982).

13. R. E. Durand and R. M. Sutherland. Growth and radiation survival characteristics of V79-171b Chinese Hamster Cells: A possible influence of intercellular contact. Radiat. Res. 56: 513-527 (1973).

14. H. Dertinger, G., Hinz and K. H. Jacobs. Intercelluar communication, 3-dimensional cell contact and radiosensitivity. Biophys. Struct. Mech. 9: 89-93 (1982).

15. H. Dertinger and D. Hulser. Increased radioresistance of cells in cultured multicell spheroids. I. Dependence on cellular interaction. Radiat. Environ. Biophys. 19: 101-107 (1981).

16. M. Guichard, H. Dertinger and E. P. Malaise. Radiosensitivity of four human tumor xenografts. Influence of hypoxia and cell-cell contact. Radiat. Res. 95: 602-609 (1983).

17. M. Haji-Karim and J. Carlsson. Proliferation and viability in cellular spheroids of human origin. Cancer Res. 38: 1457-1464 (1978).

18. J. P. Freyer and R. M. Sutherland. Selective dissociation and characterization of cells from different regions of multicell tumor spheroids. Cancer Res. 40: 3956-3965 (1980).

19. J. M. Yuhas and A. P. Li. Growth fraction as the major determinant of multicellular tumor spheroid growth rates. Cancer Res. 38: 1528=1532 (1978).

20. A. Conger and M. Ziskin. Growth of mammalian multicell tumor spheroids. Cancer REs. 43: 556-560 (1983).

21. D. F. Deen, T. Hoshino, M. Williams, I. Muraoka, K. Knebel and M. Barker. Development of a 9L rat brain tumor cell multicellular spheroid system and its response to 1,3-bis(2-chloroethyl)-1-nitrosourea and radiation. J. Natl. Cancer Inst. 64: 1373-1382 (1980).

22. T. Sasaki, M. Yamamoto, T. Yamaguchi and S. Sugiyama. Development of multicellular spheroids of HeLa cells cocultured with fibroblasts and their response to x-irradiation. Cancer Res. 44: 345-351 (1984).

23. M. L. Freeman and E. Sierra. An acidic extracellular environment reduces the fixation of radiation damage. Radiat. Res. 97: 154-161 (1984).

24. C. W. Song, J. Clement, and S. Levitt. Elimination of hypoxic protection by 5-Thio-D-glucose in multicle spheroids. Cancer Res. 38: 4499-4503 (1978).

25. B. Greider, R. F. Kallman and A. J. Franko. Recruitment of noncycling tumor cells into proliferation by isoproterenol. Cancer Res. 43: 1501-1503 (1983).

26. R. M. Sutherland, H. R. McDonald and R. L. Howell. Multicellular spheroid: a new model target for in vitro studies of immunity to solid tumor allografts: brief communication. J. Natl. Cancer Inst. 58: 1849-1853 (1977).

27. J. M. Yuhas, A. Tarleton and J. Harman. In vitro analysis of the response of multicellular tumor spheroids exposed to chemotherapeutic agents in vitro or in vivo. Cancer Res. 38: 3595-3509 (1978).

28. P. L. Olive and r. E. Durand. Penetration of AF-2 and 4NQO into multicell spheroids. Environ. Mutagenesis 5: 553-564 (1982).

29. A. Howard and S. R. Pelc. Nuclear incorporation of ^{32}p as demonstrated by autoradiographs. Exp. Cell Rs. 2: 178-187 (1951); ibid, Synthesis of deoxyribonucleic acid in normal and irradiated cells and its relation to chromosome breakage. Heredity Suppl. 6: 261-273 (1959).

30. D. M. Prescott. Reproduction of Eukaryotic Cells. Academic Press (1976).

31. E. Robbins and M. D. Scharff. The absence of a detectable G_1 phase in a cultured strain of Chinese hamster lung cell. J. Cell Biol. 34: 684-688 (1967).

32. R. Baserga. Multiplication and Division in Mammalian Cells. The Biochemistry of Disease, Vol. 6, Marcel Dekker, publ. (1976).

33. M. L. Mendelsohn. The growth fraction: a new concept applied to tumors. Science 132: 1496 (1960); ibid, Autoradiographic analysis of cell proliferation in spontaneous breast cancer of C3H mouse. III. The growth fraction. J. Natl. Cancer Inst. 28: 1015-1029 (1962).

34. L. G. Lajtha. Differential sensitivity of cell life cycle. J. Cellular Comp. Physiol. 62 (Suppl. 1): 141-156 (1963).

35. S. Gelfant. A new theory on the mechanisms of cell division. Symp. Int. Soc. Cell Biol. 2: 229-259 (1963).

36. S. Gelfant. A new concept of tissue and tumor cell proliferation. Cancer Res. 37: 3845-3962 (1977).

37. A Pardee, R. Dubrow, J. Hamlin and R. Kletzien. Animal cell cycle. Ann. Rev. Biochem. 47: 715-750 (1978).

38. C. N. Frantz. Univalent cation concentration and regulation of the Balb/c-3T3 growth cycle. In: Genetic Expression in the Cell Cycle,, K. McCarty and G. Padilla, eds. Acadmic Press, 1982.

39. J. Chafouleas, L. Lagace, W. Bolton, A. Boyd, III, and A. Means. Changes in calmodulin and its mRNA accompany re-entry of quiescent (G_0) cells into the cell cycle. Cell 36: 73-81 (1984).

40. Z. Darzynkiewicz and F. Traganos. RNA content and chromatin structure in cycling and noncycling cell population studied by flow cytometry. In: Genetic Expression in the Cell Cycle, K. McCarty and G. Padilla, eds., Academic Press (1982).

41. L. H. Augenlicht and R. Baserga. Changes in the G_0 state of W1-38 fibroblasts at different times after confluence. Exptl. Cell Res. 89: 255-262 (1974).

42. G. R. Gunther, J. Wang and G. Edelman. The kinetics of cellular commitment during stimuation of lymphocytes by lectins. J. Cell Biol. 62: 366-377 (1974).

43. H. Temin. Stimulation by serum of multiplication of stationary chicken cells. J. Cellular Physiol. 78: 161-170 (1971).

44. J. A. Smith and L. Martin. Do cells Cycle. Proc. Natl. Acad. Sci. (USA) 70: 1263-1267 (1973); R. Sheilds and J. A. Smith. Cells regulate their proliferation through alterations in transition probability. J. Cell Physiol. 91: 345-356 (1977).

45. A. B. Pardee. A restriction point for control of normal animal cell proliferation. Proc. Natl. Acad. Sci. (USA) 71: 1286-1290 (1974).

46. L. A. Dethlefsen. In quest of the quaint quiescent cells. In: Radiation Biology in Cancer Research, eds. R. Meyn and H. R. Withers. Raven Press, NY (1980).

47. O. Epifanova and V. Terskikh. On the resting periods in the cell life cycle. Cell Tiss. Kinet. 2: 75-93 (1969).

48. A. F. Hermens and G. W. Barendsen. The proliferative status and clonogenic capacity of tumour cells in a transplantable rhabdomyosarcoma of the rat before and after irradiation with 800 R x-rays. Cell Tiss. Kinet. 11: 83-100 (1978).

49. D. Grdina. Variations in radiation response of tumor subpopulations. In: Radiation Biology in Cancer Research, eds. R. Meyn and H. R. Withers, Raven Pres, NY (1980).

50. J. L. Giesbrecht, W. R. Wilson and R. P. Hill. Radiobiological studies of cells in multicellular spheroids using a sequential trypsinization techniques. Radiat. Res. 86: 368-386 (1981).

51. R. E. Durand. Isolation of cell subpopulations from in vitro tumor models according to sedimentation velocity. Cancer Res. 35: 1295-1300 (1975).

52. R. M. Sutherland and R. E. Durand. Hypoxic cells in an in vitro tumour model. Int. J. Rad. Biol. 23: 235-246 (1973).

53. G. M. Hahn and J. B. Little. Plateau-phase cultures of mammalian cells. Curr. Top. Radiat. Res. 8: 39-83 (1972).

54. M. Abercrombie and E. J. Ambrose. Cancer Res. 22: 525-548 (1962).

55. J. Ponten. Spontaneous and Virus-Induced Transformation in Cell Culture. Springer Verlag, NY, (1971).

56. K. D. Ley and R. A. Tobey. Regulation of initiation of DNA synthesis in Chinese hamster cells. J. Cell. Biol. 47: 453-459 (1970).

57. G. Sander and A. B. Pardee. Transport changes in synchronously growing CHO and L Cells. J. Cell Physiol. 80: 267-272 (1972).

58. R. E. Durand. Use of Hoechst 33342 for cell selection from multicell systems. J. Histochem. Cytochem. 30: 117-122 (1982).

59. J. Carlsson, C. G. Stalnacke, H. Acker, M. Haji-Karim, S. Nilsson and B. Larsson. The influence of oxygen on viability and proliferation in cellular spheroids. Int. J. Radiat. Oncol. Biol. Phys. 5: 2011-2020 (1979).

60. W. Mueller-Klieser and R. M. Sutherland. Influence of convection in the groth medium on oxygen tensions in multicellular tumor spheroids. Cancer Res. 42: 237-242 (1982).

61. C. J. Koch, J. Kruuv, and H. E. Frey. The effects of hypoxia on the generation time of mammalian cells. Radiat. Res. 53: 43-48 (1973).

62. C. J. Koch, J. Krucv, H. E. Frey and R. A. Snyder plateau phase in growth induced by hypoxia. Int. J. Radiat. Biol. Relat. Stud. Phys. Chem. Med. 23: 67-74 (1973).

63. R. E. Durand. Cell cycle kinetics in an in vitro tumor model. Cell Tiss. Kinet 9: 403-412 (1976).

64. E. H. Cooper, A. J. Bedford and T. E. Kenny. Cell death in normal and malignant tissues. Adv. Cancer Res. 21: 59-120 (1975).

65. Kerr and Searle. Apoptosis: its nature and kinetic role. In: Radiation Biology in Cancer Research, R. Meyn and H. R. Withers, eds., Raven Press, NY, 1980.

66. G. G. Steel. Cell loss from experimental tumors. Cell Tiss. Kinet. 1: 193 (1967).

67. A. J. Franko and R. F. Kallman. Cell loss and influx of labeled host cells in 3 transplantable mouse tumors using [^{125}I]UdR release. Cell Tiss. Kinet. 13: 381-393 (1980).

68. L. A. Dethlefsen. An evaluation of radio-iodine-labelled 5-iodo-2'-deoxyuridine as a tracer for measuring cell loss from solid tumors. Cell Tiss. Kinet. 4: 123 (1971).

69. S. B. Curtis, G. W. Barendsen and A. F. Hermens. Cell kinetic model of tumour growth and regression for a rhabdomyosarcoma in the rat. Undisturbed growth and radiation response to large single doses. Eur. J. Cancer 9: 81-88 (1973).

70. J. Landry, J. P. Freyer and R. M. Sutherland. A model for the growth of multicellular spheroids. Cell Tiss. Kinet. 15: 585-594 (1982).

71. D. L. S. McElwain and P. J. Ponzo. A model for the growth of a solid tumor with non-uniform oxygen concentration. Math. Biosci. 34: 267-279 (1977).

72. E. Frindel, E. P. Malaise, E. Alpen and M. Tubiana. Kinetics of cell proliferation of an experimental tumor. Cancer Res. 27: 1122-1131 (1967).

73. J. Landry, J. P. Freyer, and R. M. Sutherland. Shedding of mitotic cells from the surface of multicell spheroids during growth. J. Cell Physiol. 106: 23-32 (1981).

74. J. Searle, D. J. Collins, B. Harmon, and J. F. R. Kerr. The spontaneous occurrence of apoptosis in squamous carcinomas of the uterine cervix. Path. 5: 163-169 (1973).

75. A. J. Franko and R. M. Sutherland. Oxyen diffusion distance and development of necrosis in multicell spheroids. Radiat. Res. 79: 439-453 (1979).

76. A. J. Franko and R. M. Sutherland. Rate of death of hypoxic cells in multicell spheroids. Radiat. Res. 76: 561-572 (1978).

77. EW. Mueller-Klieser, J. P. Freyer and R. M. Sutherland. Evidence for a major role of glucose in controlling development of necrosis in EMT6/R_0 multicell tumor spheroids. Adv. Exp. Med. Biol. 159: 487-496 (1982).

78. C. K. N. Li. The role of glucose in the growth of 9L multicell tumor spheroids. Cancer 50: 2074-2078 (1982).

79. C. Ceccarini and H. Eagle. pH as a determinant of cellular growth and contact inhibition. Proc. Natl. Acad. Sci. (USA) 68: 229-233 (1971).

80. J. Wigle, J. Freyer, and R. M. Sutherland. Use of a sedimentation column to obtain uniformly-sized populations of multicell spheroids. In Vitro, in press (1983).

81. H. G. Crabtree. Observation of the carbohydrate metabolism of tumors. Biochem. J. 23: 536-541 (1929).

82. R. B. Painter. The role of DNA damage and repair in cell killing induced by ionizing radiation. In: Radiation Biology in Cancer Research, R. Meyn and H. R. Withers, eds., Raven Press, NY, 1980.

83. K. H. Chadwick and H. P. Leenhouts. A molecular theory of cell survival. Phys. Med. Biol. 13: 78-87 (1973).

84. C. A Tobias, E. A. Blakely, F. Ngo, T. Yang. The repair-misrepair model of cell survival. In: Radiation Biology in Cancer Research, R. Meyn and H. R. Withers, eds., Raven Press, NY, 1980.

85. M. M. Elkind and H. Sutton. Radiation response of mammalian cells grown in culture. I. Repair of X-ray damage in surviving Chinese hamster cells. Radiat. Res. 13: 556-593 (1960).

86. M. M. Elkind and G. F. Whitmore. The Radiobiology of Cultured Mammalian Cells. Gordon and Breach, NY, 1967.

87. J. E. Cleaver. DNA repair and its coupling to DNA replicatin in eukaryotic cells. Biochem. Biophys. Acta 516: 489-516 (1978).

88. R. A. Phillips and L. J. Tolmach. Repair of potentially lethal damage in x-irradiated HeLa cells. Radiat. Res. 29: 413-432 (1966).

89. J. B. Little, G M. Hahn, E. Frindel and M. Tubiana. Repair of potentially lethal radiation damage in vitro and in vivo. Radiology 106: 689-694 (1973).

90. G. M. Hahn, M. A. Bagshaw, R. G. Evans and L. F. Gordon. Repair of potentially-lethal lesions in x-irradiated, density-inhibited Chinese hamster cells, metabolic effects and hypoxia. Radiat. Res. 55: 280-290 (1973).

91. H. Suit and M. Urano. Repair of sublethal radiation injury in hypoxic cells of a C3H mouse mammary carcinoma. Radiat. Res. 37: 423-434 (1969).

92. T. Terasima and L. J. Tolmach. Variatios in several responses of HeLa cells to x-irradiation during the division cycle. Biophys. J. 3: 11-33 (1963).

93. B. F. Kimler and S. D. Henderson. Cyclic responses of cultured 9L cells to radiation. Radiat. Res. 91: 155-168 (1982).

94. P. Keng and K. T. Wheeler. Radiation response of synchronized 9L rat brain tumor cells separatd by centrifugal elutriation. Radiat. Res. 83: 633-643 (1980).

95. M. M. Elkind, R. W. Swain, T. Alescio, H. Sutton, W. B. Moses. Oxygen nitrogen, recovery and radiation therapy. In: Cellular Radiation Biology, Williams and Wilkins, Baltimore, 1965.

96. S. B. Curtis and T. Tenforde. Assessment of tumour response in a rat rhabdomyosarcoma. Br. J. Cancer 41 (Suppl. IV): 266-270 (1980).

97. Y. Doida and S. Okada. Radiation-induced mitotic delay in cultured mammalian cells (L5178Y). Radiat. Res. 38: 513-529 (1969).

98. M. Collyn-d'Hooghe, D. Hemon, R. Gilet, S. B. Curtis, A. J. Valleron and E. P. Malaise. Comparative effects of ^{60}Co γ-rays and neon and helium ions on cycle duration and division probability of EMT6 cells. A time-lapse cinematography study. Int. J. Radiat. Biol. 39: 297-306 (1981).

99. J. H. Kim and T. C. Evans. Effects of x-irradiation on the mitotic cycle of ehrlich ascites tumor cells. Radiat. Res. 21: 129-143 (1964).

100. G. F. Whitmore, J. E. Till and S. Gulyas. Radiation induced mitotic delay in L cells. Radiat. Res. 30: 155-171 (1967).

101. D. B. Leeper, M. H. Schneiderman, and W. C. Dewey. Radiation induced division delay in synchronized Chinese hamster ovary cells in monolayer culture. Radiat. Res. 50: 401-417 (1972).

102. R. L. Warters and K. G. Hofer. Radionuclide toxicity in cultured mammalian cells. Elucidation of the primary site for radiation-induced division delay. Radiat. Res. 69: 348-359 (1977).

103. M. H. Schneiderman and K. G. Hofer. The target for radiation-induced division delay. Radiat. Res. 84: 462-476 (1980).

104. D. O. Schneider and R. M. Johns. Enhancement of radiation-induced mitotic inhibition by BUdR incorporation in L-cells. Radiat. Res. 28: 657-667 (1966).

105. M. M. Elkind, A. Han and K. W. Volz. Radiation response of mammalian cells grown in culture IV. Dose-dependence of division delay and post-irradiation growth of surviving and non-surviving Chinese hamster cells. J. Natl. Cancer Inst. 30: 705-721 (1963).

106. T. Munro. The site of the target region for radiation-induced mititoc delay in cultured mammalian cells. Radiat. Res. 44: 748-757 (1970).

107. E. N. Brewer and N. Oleinick. Histore phosphorylation during radiation-induced mitotic delay in synchronous plasmodia of physarum polycephalum. Int. J. Rad. Biol. 38: 697-702 (1980).

108. S. Mak and J. E. Till. The effects of x-rays on the progress of L-cells through the cycle. Radiat. Res. 20: 600-618 (1963).

109. R. E. Durand and P. L. Olive. Radiation-induced DNA damage in V79 spheroids and monolayers. Radiat. Res. 78: 50-60 (1979).

110. I. Korner, et al. Stud. Biophys. 68: 161 (1978).

111. R. E. Durand and R. M. Sutherland. Effects of intercellular contact on repair of radiation damage. Exptl. Cell Res. 71: 75-80 (1972).

112. R. E. Durand. Variable radiobiological responses of spheroids. Radiat. Res. 81: 85-99 (1980).

113. R. E. Durand and R. M. Sutherland. Intercellular contact: its influence on the Dq of mammalian cell survival curves. In: 6th L. H. Gray Conference Proc. John Wiley and Sons, London (1975).

114. C. A. Wallen, S. Michaelson and K. T. Wheeler. Evidence for an unconventional radiosensitivity of rat 9L subcutaneous tumors. Radiat. Res. 84: 529-541 (1980).

115. R. Durand and R. Sutherland. Cancer Res. 32: 2587 (1972).

116. R. Azarnia and W. Larsen. In: Intercellular Communication; W. C. DeMello, ed. Plenum Press, New York (1977).

117. J. Pitts and M. Finbow, also In: Intercellular Communication, W. C. DeMello, ed. Plenum Press, New York (1977).

118. J. S. Rasey. Cell-cell contact and repair of radiation damage. In: Proc. 7th Int'l Congress of Radiat. Res. pp. 303-310. J. Broerse et al., eds., Martinus Nijhoff, publ. (1983).

119. A. Rodriguez and E. Alpen. Feeder cells and cell survival in spheroids and monolayers. Int. J. Radiat. Biol. 41: 111-117 (1982).

120. A. J. Franko and R. M. Sutherland. Radiation survival of cells from spheroids grown in different oxygen concentrations. Radiat. Res. 79: 454-467 (1979).

121. R. E. Durand. Oxygen enhancement ratio in V79 spheroids. Radiat. Res. 96: 322-334 (1983).

122. A. J. Franko and C. J. Koch. The radiation response of hypoxic cells in EMT6 spheroids in suspension culture does model data from EMT6 tumors. Radiat. Res. 96: 497-504 (1983).

123. J. T. Leith, W. Schilling and K. T. Wheeler. Cellular radiosensitivity of a rat brain tumor. Cancer 35: 1545-1550 (1975).

124. K. T. Wheeler, M. Barker, C. A. Waller, B. F. Kimler and S. Henderson. Evaluation of 9L as a brain tumor model. Manuscript, 1981.

125. R. E. Durand and R. M. Sutherland. Dependence of the radiation response of an in vitro tumor model on cell cycle effects. Cancer Res. 33: 213-219 (1973).

126. R. E. Durand and J. E. Biaglow. Radiosensitization of hypoxic cells of an in vitro tumor model by respiratory inhibitors. Radiat. Res. 69: 359 (1977).

127. H. Dertinger and A. Seiter. Split-dose survival and cycle progression of proliferating and non-proliferating cells in V79 spheroids. Int. J. Radiat. Biol. 31: 401-403 (1977).

128. H. Dertinger and C. Lucke-Huhle. A comparative study of post-irradiation growth kinetics of spheroids and monolayers. Int. J. Radiat. Biol. 28: 255-265 (1975).

129. C. Lucke-Huhle, E. A Blakely, F. Ngo, P. Chang and C. A. Tobias. Survival and kinetic response of V79 spheroids after exposure to heavy ion beams. Int. J. Radiat. Biol. 37: 483-492 (1980).

130. A. Rodriguez and E. L. Alpen. Cell survival in spheroids irradiated with heavy-ion beams. Radiat. Res. 85: 24-37 (1981).

131. Y. Sano, T. Hoshino, M. Barker and D. F. Deen. Response of 9L rat brain tumor multicellular spheroids to single and fractionated doses of 1,3-bis(2-choroethyl)-1-nitrosourea. Cancer Res. 44: 571-576 (1984).

132. J. E. Cleaver. Thymidine metabolism and cell kinetics. North-Holland Publishing co., Amsterdam, 1967.

133. J. Yuhas, A. P. Li, A. O. Martinez, and A. J. Landman. A simplified method for production and growth of multicellular tumor spheroids. Cancer Res. 37: 3639-3643 (1977).

134. J. M. Yuhas, A. E. Tarleton, and K. Molzen. Multicellular tumor spheroid formation by breast cancer cells isolated from different sites. Cancer Res. 38: 2486-2491 (1978).

135. Error in numbering; no such reference in text.

136. S. Rockwell and R. F. Kallman. Growth and cell population kinetics of single and multiple KHT sarcoma. Cell Tissue Kinet. 5: 449-457 (1972).

137. T. E. Hamilton and J. Dobbin. The percentage labelled mitoses technique shows the mean cell cycle time to be half its true value in carcinoma NT. Cell Tissue Kinet. 16: 473-492 (1983).

138. A. C. Begg. Cell loss from several types of solid murine tumour:comparison of [^{125}I]iododeoxyuridine and tritiated thymidine methods. Cell Tissue Kinet. 10: 409 (1977).

139. P. Ross-Riveros. The effects of elevated temperatures on cell cycle kinetics of rat gliosarcoma cells. Ph.D. Thesis, University of California, Berkeley (1978).

140. J. M. Yuhas, A. P. Li, A. Martinez and A. Ladman. A simplified method for production and growth of multicellular tumor spheroids. Cancer Res. 37: 3639-3643 (1977).

141. A. J. Franko and R. F. Kallman. Cell loss and influx of labeled host cells in three transplantable mouse tumors using [^{125}I]UdR release. Cell Tissue Kinet. 13: 381-393 (1980).

142. G. W. Hathaway. Thermotolerance in 9L-gliosarcoma cells. Ph.D. Dissertation, University of California, Berkeley (1982).

143. C. Lucke-Huhle, E. A. Blakely, P. Chang and C. A. Tobias. Drastic G_2 arrest in mammalian cells after irradiation with heavy-ion beams. Radiat. Res. 79: 97-112 (1979).

144. S. E. Shackney and S. S. Ford. Correlations between the DNA content distribution and tritiated thymidine studies in relation to population size in sarcoma 180 in vitro. Cancer Res. 39: 1401-1407 (1974).

145. R. Rowley, M. Zorch and D. B. Leeper. Effect of caffeine on radiation-induced mitotic delay: delayed expression of G_2 arrest. Radiat. Res. 97: 178-185 (1984).

146. F. Zampetti-Bosseler and D. Scott. Cell death chromosome damage and mitotic delay in normal human ataxia telangiectasia and retinoblastoma fibroblasts after x-irradiation. Int. J. Radiat. Biol. 39: 547-558 (1981).

147. M. D. Ford, L. Martin and M. F. Lavin. The effects of ionizing radiation on cell cycle progression in ataxia telangiectasia. Mutat. Res. 125: 115-122 (1984).

148. R. B. Painter and B. R Young. Radiosensitivity in ataxia-telangiectasia. A new explanation. Proc. Natl. Acad. Sci. USA 77: 7315-7317 (1980).

149. P. M. Busse, S. K. Bose, R. W. Jones and L. J. Tolmach. The action of caffeine on x-irradiated HeLa cells. III. Enhancement of x-ray killing during G_2 arrest. Radiat. Res. 76: 292-307 (1978).

150. D. R. Miller, W. C. Dewey and H. Miller. X-ray induced delay in the Chinese hamster cell-cycle: dependence on phase irradiated under different culturing conditions, BUdR incorporation, and hypertonic treatment. Int. J. Radiat. Biol. 23: 591-602 (1973).

151. S. C. vanAnkeren and K. T. Wheeler. Relationship between the repair of radiation-induced DNA damage and recovery from potentially-lethal damage in 9L rat brain tumor cells. Cancer Res. 44: 1091-1097 (1984).

152. J. W. Daniel and N. L. Oleinick. Cyclic nucleotide responses and radiation-induced mitotic delay in Physarum polycephalum. Radiat. Res. 97: 341-351 (1984).

153. S. E. Shackney, S. S. Ford and A. B. Wittig. The effects of counting threshold and emulsion exposure duration on the pulse-labelled mitosis curve and their implications for cell cycle analysis. Cancer Res. 33: 2726-2731 (1973).

154. P. Twentyman and J. M. Yuhas. Use of a bacterial neutral protease for disaggregation of mouse tumors and multicellular tumor spheroids. Cancer Letters 9: 225-228 (1980).

155. C. Lucke-Huhle. Alpha-irradiation induced G_2 delay: a priod of cell recovery. Radiat. Res. 89: 298-308 (1982).

156. S. Lehnert. Relationship of cyclic AMP levels to duration of radiation-induced mitotic delay. Int. J. Radiat. Biol. 36: 417-422 (1979).

157. A. Rodriguez. Abstract No. Hg-4, 32nd Annual Rad. Res. Meeting, March 1984.

FIGURE LEGENDS

Fig. 1. Rate of increase of spheroid cell number over 24 days in spinner culture. Open symbols: cells/ml of culture medium controlled to be ~1.5 x 10^5 cells/ml. Closed symbols: cells/ml of medium not controlled, reaching 10^6 cells/ml by day 11. Medium changed daily for both culture conditions, beginning at day 2 of culture. T_D in hours for spheroids of various diameters obtained by estimating a tangent to the curve at points corresponding to the appropriate spheroid diameter.

Fig. 2a. Rate of increase of spheroid diameter over 24 days in spinner culture. Data points from cell density controlled cultures only.

Fig. 2b. Relationship of spheroid cell number to spheroid volume. Data points from all experiments shown in Fig. 1 plus additional experiments.

Fig. 3. Pulse-labelled mitoses curves.

Fig. 3a. PLM curve for 9L cells grown as monolayers. 48 hours after seeding, with 1 x 10^5 cells, replicate 25 cm^2 flasks were pulse-labelled for 15 minutes with ^{3}H-thymidine, then harvested at subsequent intervals.

Fig. 3b and 3c PLM curves for 9L cells grown as spheroids. b. 400 μm spheroids pulse-labelled for 20 minutes. c. 800 μm spheroids pulse-labelled for 30 minutes.

Fig. 4. Radiation survival of noncycling cells in spheroids compared to that of the whole spheroid cell population. Closed symbols: spheroids treated with high-specific activity ^{3}H-thymidine to kill all cycling cells prior to irradiation, corrected for killing by the suicide treatment. Open symbols: spheroids not given ^{3}H-thymidine prior to irradiation. Different symbols refer to different radiation doses. Error bars indicate standard deviations of the mean.

Fig. 5. Radiation-induced Division Delay, 500 rad.

Fig. 5a. Pulse-labelled mitoses curves for 9L monolayes given 0 rad and 500 rad x-rays, respectively. Dashed line shows control (0 rad) curve from Fig. 3a. ΔG_2 is the difference in the length of time required for curves from irradiated and unirradiated cells to reach the half-height of the first peak of labelled mitoses.

Fig. 5b. PLM curves for 800 μm 9L monolayers given 0 rad and 500 rad of x-rays, respectively. Dashed line represents control (0 rad) curve from Fig. 3c. ΔG_2 defined as for Fig. 5a.

Fig. 6. Radiation-induced division delay, 800 rad.

Fig. 6a. PLM curves for 9L monolayers given 0 rad and 800 rad of x-rays, respectively. Dashed line shows control (0 rad) curve from Fig. 3a. ΔG_2 is the difference in time required for curves from irradiated and unirradiated cells to reach the half-height of the first peak of labelled mitoses.

Fig. 6b. PLM curves for 800 μm 9L spheroids given 0 rad and 800 rad x-rays, respectively. ΔG_2 defined as for fig. 6a.

Table I. Measurements of spheroid grown fraction for spheroids of various sizes. Left hand column: labelling-index after 12 hours of continuous labelling with ^{3}H-thymidine: mean and standard deviation of 3 to 5 experiments per point. Right-hand column: GF derived from pulse-labelled mitosis experiments: L.I. population/L.I. proliferating cells, where L.I. proliferating = T_s/T_c.

Table II. Rate of shedding of cells from spheroids of 3 different diameters. Expressed as number of cells per spheroid per hour, and as percent of total spheroid cell number per hour (farthest-right column).

Table III. Compiled kinetic parameters of spheroids. GF_1 = growth fractions (GF's) measured by 12 hours continuous labelling (from Table I)). GF_2 = GF's derived from PLM experiments (also from Table I)., GF_{est} = GF_s estimated from the 12 hr continous labelling data corrected for the fraction of 'missed' cells (see Discussion). T_D's estimated by tangents to growth curve (see Fig. 1). T_c: estimated from PLM curves for monolayer, 400 μm and 800 μm spheroids, only. For spheroids of other sizes, the upper and lower limits of T_c are given. For spheroids 100-150 μm, T_c is assumed to be the same as for monolayers. ϕ, cell loss factor: calculated for several estimates of GF and T_c (see Appendix). Upper and lower limits given.

K_L = rate of loss derived as in Appendix, expressed as percent of total spheroid cell number per hour.

Spheroid Growth Rate

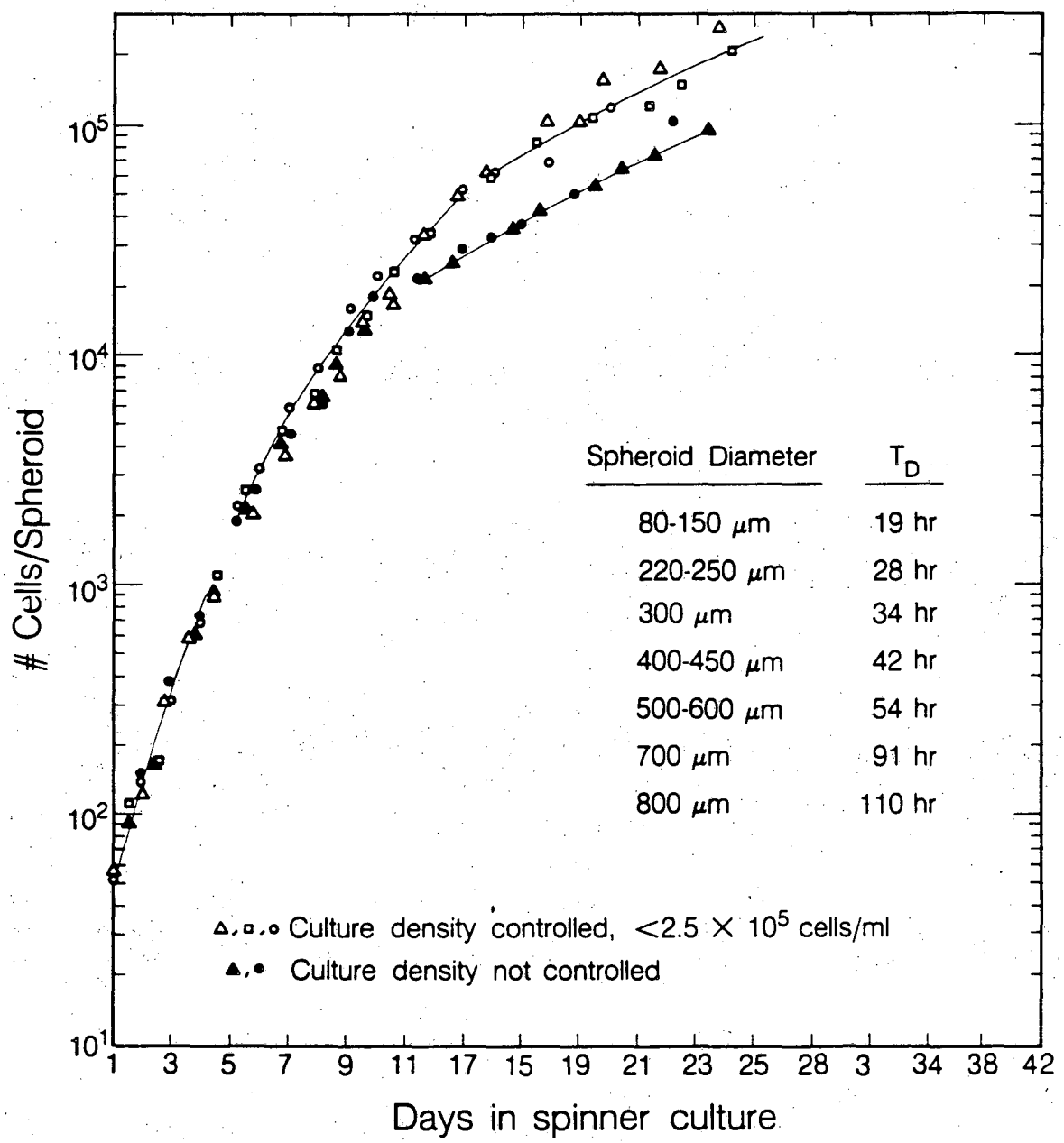

Fig. 1

XBL 843-7668

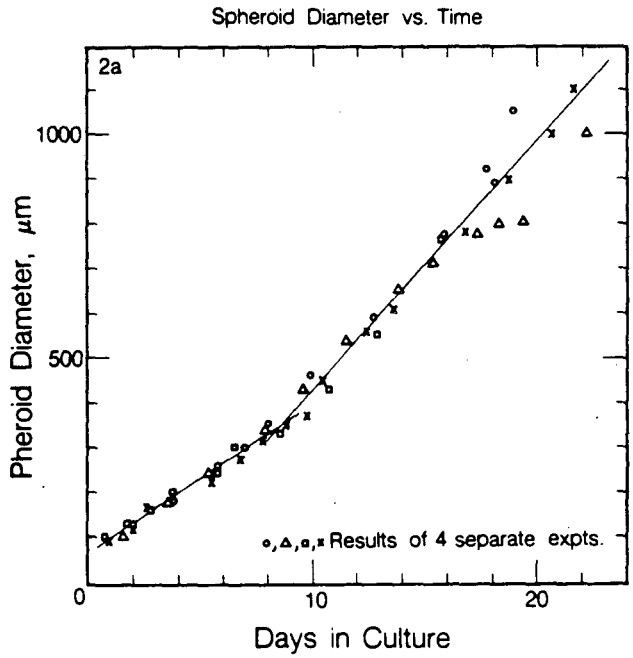

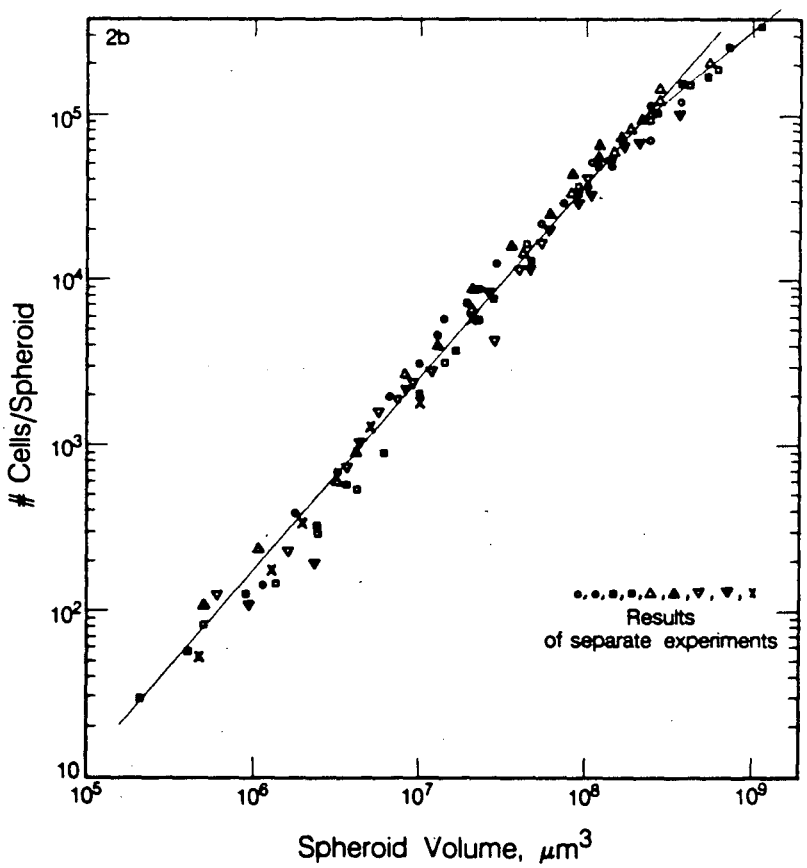

Fig. 2

XBL 843-7670-A

Percent labelled mitoses curves

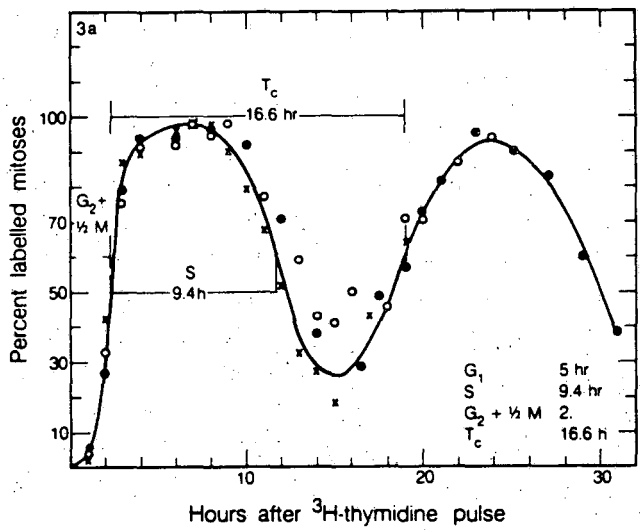

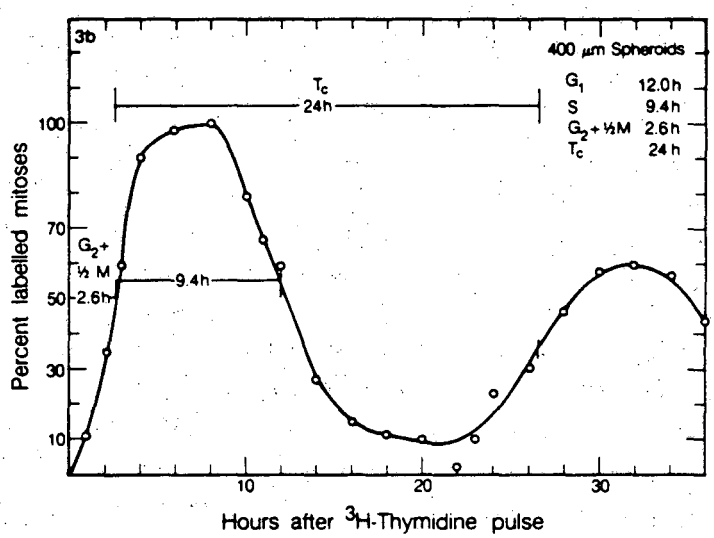

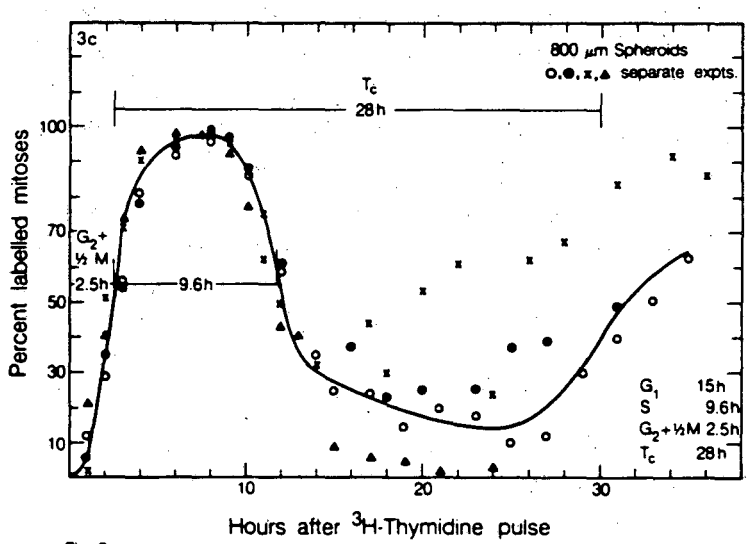

Fig. 3

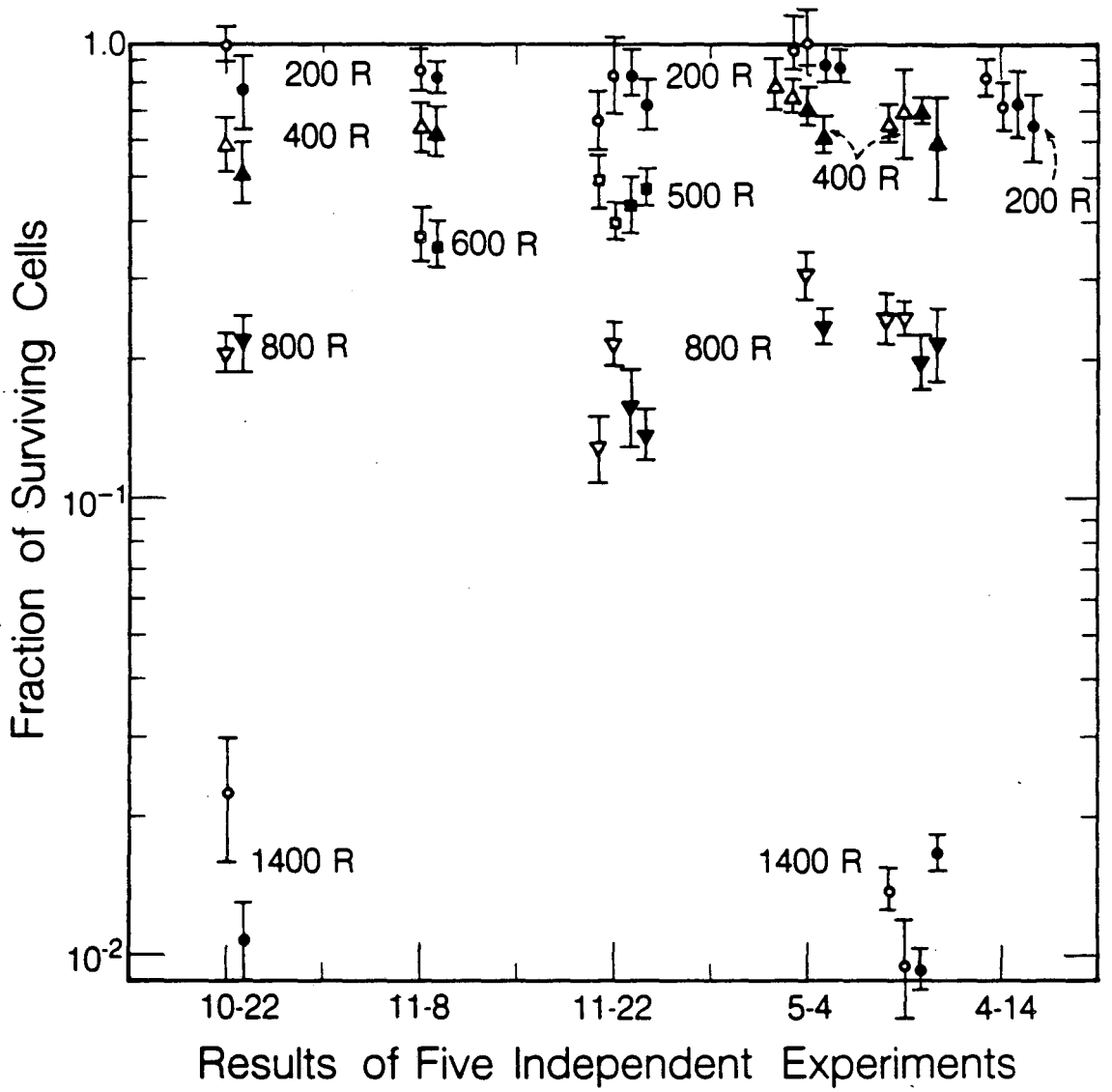

Open Symbols: Irradiated Controls
Closed Symbols: Suicide-Treated and Irradiated

Fig. 4

XBL 843-7669

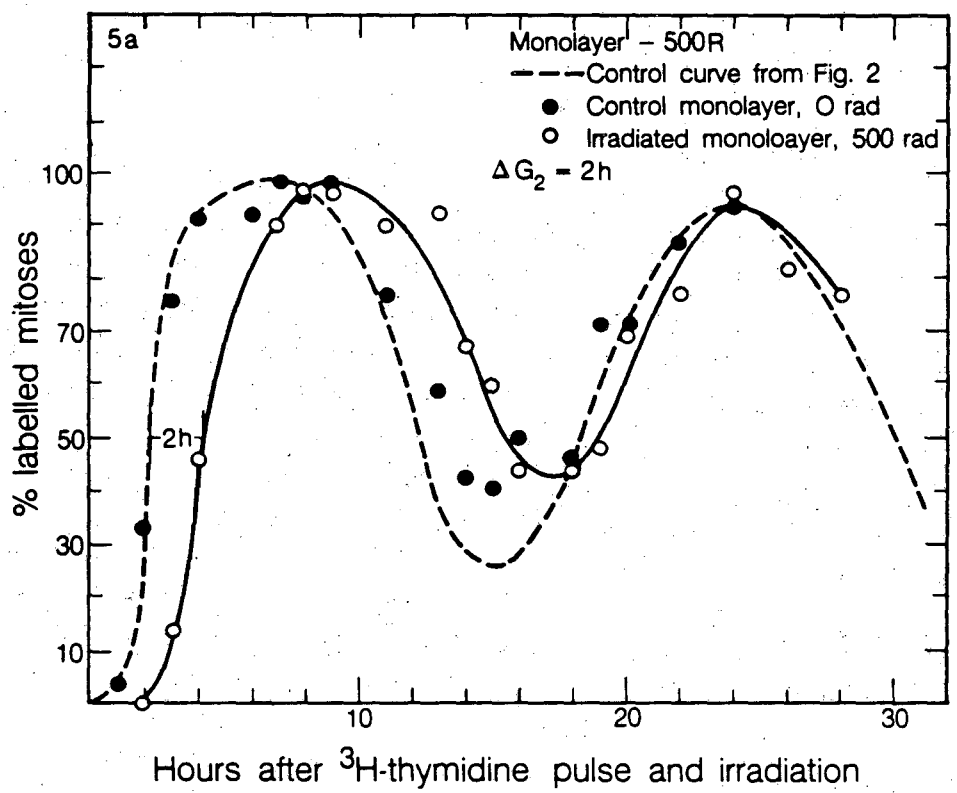

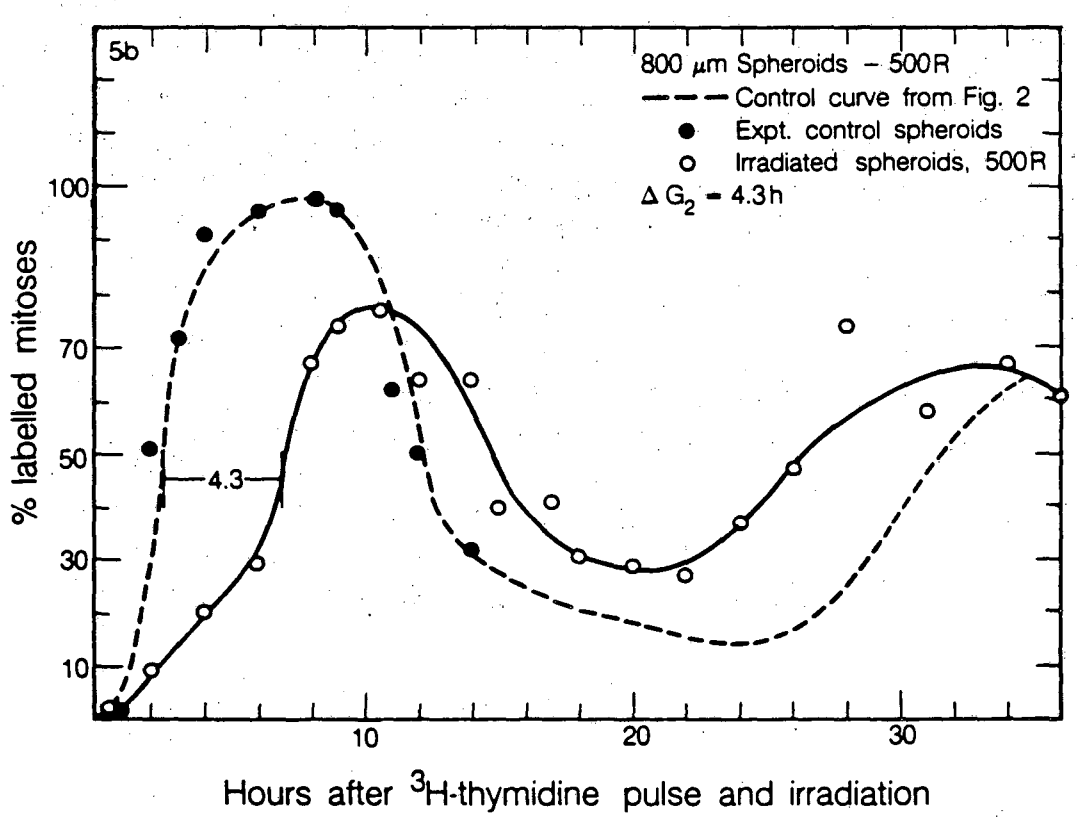

Fig. 5

XBL 843-7663-A

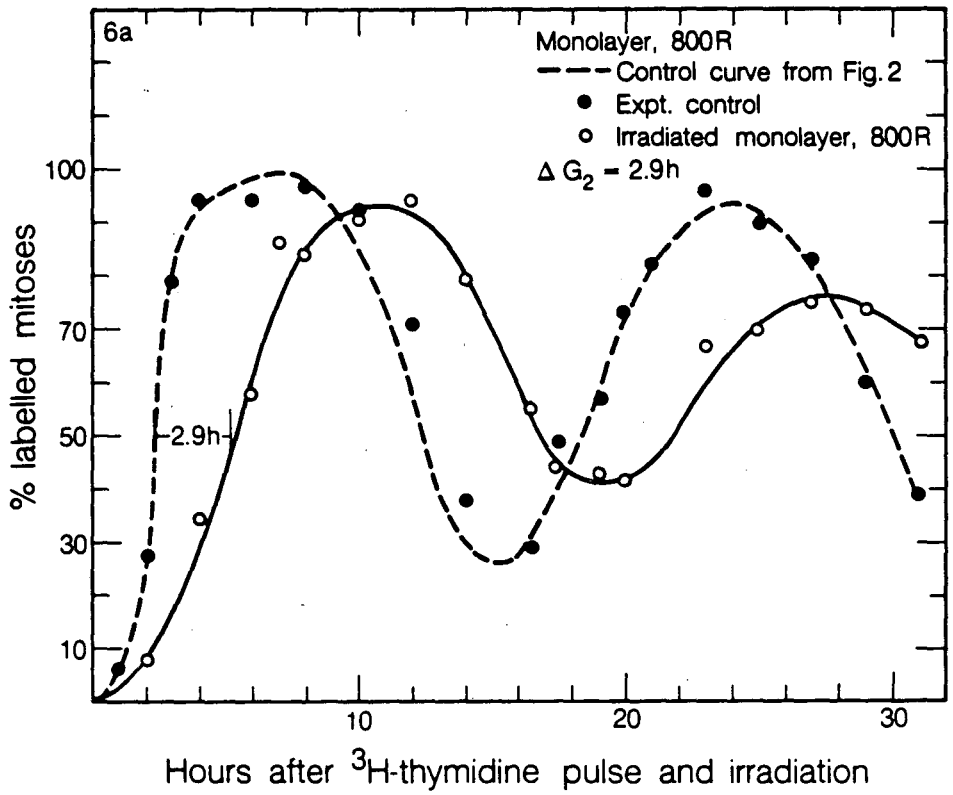

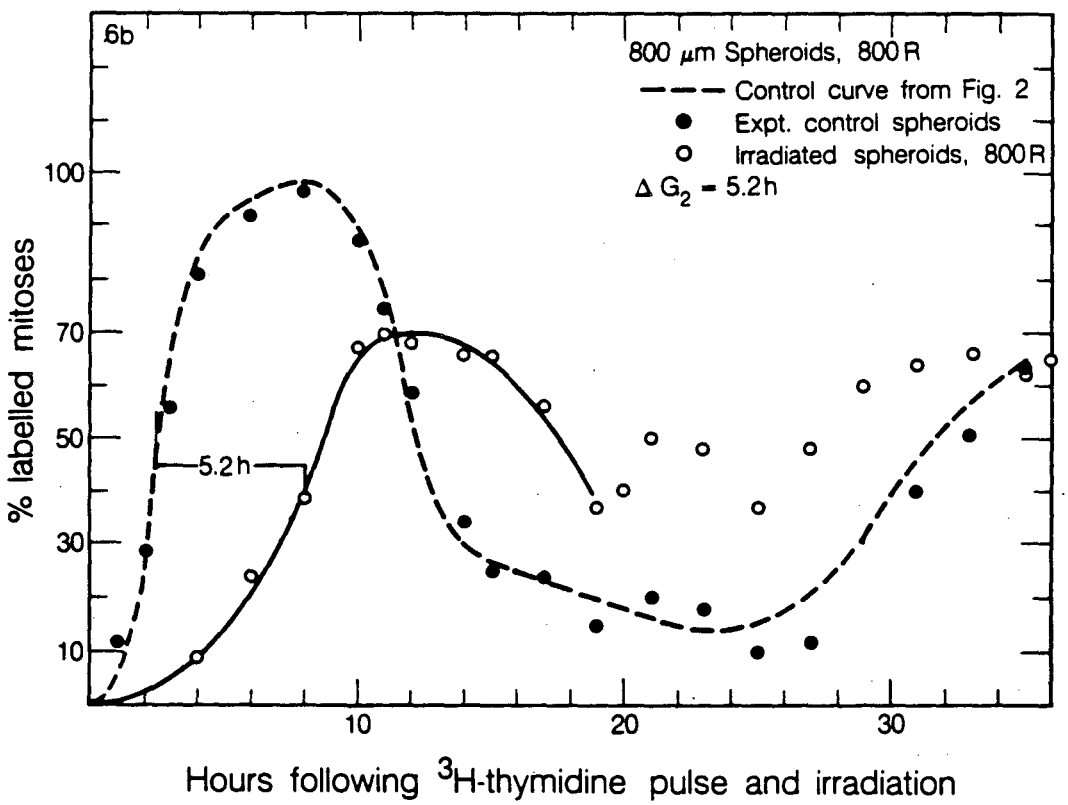

Fig. 6

XBL 843-7686-A

Table I

Spheroid Size	Growth Fraction 12 hours-continuous label	Growth Fraction from PLM data
150 μm	.86 ± .046	
220-250 μm	.69 ± .073	
300 μm	.57 ± .04	
400-450 μm	.49 ± .03	.67
500-600 μm	.43 ± .03	
800-850 μm	.40 ± .03	.50 ± .059
Monolayer	0.97	.89 ± .05

Table II

Spheroid Size	Expt #	Rate of Cell Shedding: Percent of Spheroid Cells/sph-hour		per hour
300 μm	10-14	3.97 6.42	5.2 ± 1.73	.07%/hr
	12-9	3		
500 μm	10-14	34.5 33.5	34 ± 0.71	.113%/hr
	11-12	15.4 14.0	14.7 ± 1	.05%/hr
800 μm	10-21	184 268	226 ± .59	.19%/hr
	5-5	145 99	122 ± 33	.10%/hr

Table III.
Compiled Kinetic Parameters of Spheroids

Diameter	GF_1	GF_2	$GF_{est.}$	T_D	T_C	ϕ	K_L
100-150 μm	.86 ± .046			19 h	16.6 hr		
220-250 μm	.69 ± .073			28 h	16.6 h	0.14	
					24 h	< 0	
300 μm	.57 ± .04			34 h	24 h	< 0	
			.65		24 h	< 0	
400-450 μm	.49 ± .03			42 h	24 h	< 0	
		.67			24 h	.15	.2%/hr
			.56		24 h	< 0	
500-600 μm	.43 ± .03			54 h	24 h	< 0	
			.56		28 hr	.07	.1%/hr
800-850 μm	.40 ± .03			110 h	28 hr	.36	
		.50 ± .06			28 hr	.51	
			.51		28 hr	.50	0.7%/hr

This report was done with support from the Department of Energy. Any conclusions or opinions expressed in this report represent solely those of the author(s) and not necessarily those of The Regents of the University of California, the Lawrence Berkeley Laboratory or the Department of Energy.

Reference to a company or product name does not imply approval or recommendation of the product by the University of California or the U.S. Department of Energy to the exclusion of others that may be suitable.

TECHNICAL INFORMATION DEPARTMENT
LAWRENCE BERKELEY LABORATORY
UNIVERSITY OF CALIFORNIA
BERKELEY, CALIFORNIA 94720